Česká zemědělská univerzita v Praze
Czech University of Life Sciences, Prague

Fakulta Agrobiologie, Potravinových a Přírodních zdrojů
Katedra Agroekologie a Biometeorologie

Universität für Bodenkultur Wien
University of Natural Resources and Life Sciences, Vienna

Department Wasser-Atmosphäre-Umwelt
Institut für Hydraulik und Landeskulturelle Wasserwirtschaft

Natural Resources and Environment, CULS & Natural Resources Management and Ecological Engineering, BOKU

Estimation of the actual maize crop water consumption by different methods and their comparison

Double Degree diploma thesis

Author: Zuzana Galajdová, BSc.

Supervisors: Dr. Ing. Jan Pivec, CULS Prague, Czech Republic

Ass. Prof. Dipl.-Ing. Dr. nat. techn. Peter Cepuder, BOKU Vienna, Austria

Declaration

I hereby declare that I have elaborated this Master Thesis on my own, and have not used sources or means without declaration in the text. Any thoughts from others or literal quotations are clearly marked and all explanations that I copied directly or in their sense are marked as such, as well as the thesis has not yet been handed in neither in this nor in equal form at any other official commission. Furthermore, I agree to an anonymous test of plagiarism which electronically verifies the validity of my declarations.

Acknowledgement

Foremost, I would like to express my sincere gratitude to my supervisor Dr. Ing. Jan Pivec, for his continuous support of my master studies and research, for his motivation and enthusiasm. His guidance was helpful during the whole time of writing my thesis. I could not have imagined having a better advisor and mentor for my MSc. studies. I would like to thank to my co-supervisor Ass.Prof. Dipl.-Ing. Dr.nat.techn Peter Cepuder for his willingness and patience.

Besides my supervisors, I would like to thank to Ing. Václav Brant, Ph.D., Ing. Hana Vostrá-Vydrová, Ing. Christopher Ash and João Barradas, MSc. for their valuable expert advice.

My sincere thanks also go to my friends who support me and to my cat Nessie, the endless source of positive energy.

Last but not least, I would like to thank to my family – to my grandpa Ing. Emanuel Boubelík, who is my greatest inspiration, to my parents, for giving me birth and for supporting me throughout my life and to my boyfriend for his understanding, encouragement and unconditional love.

Preface

This thesis is submitted to Czech University of Life Sciences Prague, Faculty of Agrobiology, Food and Natural Resources, Department of Agroecology and Biometeorology and to the University of Natural Resources and Life Sciences Vienna, Department of Water, Atmosphere and Environment, Institute of Hydraulics and Rural Water Management in partial fulfilment of the requirements for the Double Degree of Master of Science in Natural Resources and Environment and Natural Resources Management and Ecological Engineering.

Abstract

Estimation of maize crop water consumption by different methods and their comparison

Summary: The mechanism of the water motion in plant is based on the creation of negative pressure in the leaf tissues due to unique physical properties of water. The comparison of the BREB and sap slow methods showed, that both methods are suitable for the estimation of the evaporation. Diverse plant forms can have any combination of a large hydraulic resistance and large hydraulic capacitance. When estimating the sap flow for the whole canopy, it has to be taken into an account, that upscalling from leaf to plant canopy is difficult to do because measurements with these methods reflect only reactions of single plants. Even though some issues associated with upscalling from the leaf into the whole canopy exist, there is the possibility to estimate the water consumption of the plants.

In this work we focused on one part of hydrological cycle. This process is called evapotranspiration. Assuming, 100% of water participating on hydrological cycle, 12.3% of this amount of water is evaporated from the continents back to the troposphere. For the measurements was chosen the corn plant (*Zea mays L.*). As corn is the most productive crop plant that originated in western hemisphere, but after the discovery of the Western world in 1492, corn has spread rapidly and is grown in nearly all areas of the world. Corn belongs among the top most grown crops worldwide. Its production sustains important source for food and forage production. For thousands years, corn has been accompanying humans who further cultivated it, and thereby the corn participated on the process of the formation of the cultural patterns and habits of many ethnics.

Keywords: Bowen ratio energy balance, sap flow, maize, water consumption, evapotranspiration, Penman-Monteith equation

Table of Contents

1 Introduction

Water covers most of the Earth's surface and keeps the temperature fluctuations within the limits convenient for life. Agriculture, industry and growing population in cities mutually compete through the political influences for water. Theories how to attempt for the agreement within the groups of the various interests are as well as important as understanding the natural resources management. Key to the economical and ecological water use is to integrate science, technology and society knowledge and put the priorities in a rational order. Crop evapotranspiration refers to the amount of water which is lost through evapotranspiration; Crop water requirement refers to the amount of water that needs to be supplied. The irrigation water requirement basically represents the difference between the crop water requirement and effective precipitation. Limited water resources in arid regions, soil salinization and pollution, are the reasons for searching for more sustainable and effective water sources. The evapotranspiration process is determined by the amount of energy available to vaporize water. Fluxes along the soil-plant-atmosphere continuum are regulated by above ground plant features like the leaf stomata, which can regulate plant transpiration when interacting with the atmosphere and plant root-system properties such as depth, distribution and activity of roots, as well as soil properties like the soil water retention and hydraulic conductivity characteristics. This work will focus more on the relationship between atmosphere and plant measurement techniques such as the sap flow method which continuously monitor whole plant physiology and the Bowen-Ratio energy balance method.

Motivation for this work is to widen the knowledge about the water exchange balance between the canopy and the ambient atmosphere. Evaporation and evapotranspiration play important roles in the hydrological cycle. This work may contribute to better understanding and consequently increase the interest in research of the water use efficiency which could thereby contribute to mitigation of energy and economical losses in agriculture.

2 Literature review

2.1 Water and its characteristics

2.1.1 Molecular composition of water

Water is a biological medium which enables the life. All the organisms related to humans consist mostly of water; water also dominates to the environment in which they live. Life on the Earth started in water and has been evolving 3 billion years before the expanding to the continents. Modern life, even the terrestrial one is closely linked with water. Most of the cells are surrounded by water and the cells themselves are composed of 70-90 % by water. Water is present on three fifths of the Earth's surface and it is the only common substance occurring under natural conditions in all three phases - liquid, solid (ice) or gas (vapour).

A molecule of water consists of two hydrogen atoms connected to the oxygen atom by a single covalent bond. The water molecule has a wide opened V- shape. It is a polar molecule which means that opposite ends of the molecule have opposite charges. As the oxygen is more electronegative than the hydrogen, electrons of the polar bonds spend more time in proximity of the oxygen atom. The area of the molecule in proximity of the oxygen has the negative partial charge and the area close to hydrogen atoms has the positive partial charge.

2.1.1.1 Hydrogen bonds and cohesive forces

When water is in liquid form, its hydrogen bonds are very fragile. They are created, disintegrated and created again very quickly. Each hydrogen bond lasts only a few trillionths of a second, but the molecules create new bonds with new partners. In each moment a significant amount of molecules create a bond with their neighbours. That is what gives water greater structural orderliness than to other liquids. This phenomenon when the hydrogen bonds hold the molecules together is called cohesion.

Cohesive forces, together with adhesion of water to the vessel walls, contribute to the transport of water against the gravity in plants. Water enters to the leaves trough microscopic veins which lead from the roots. Water evaporated from the leaves is being replaced in leaf-vessels by the water from the veins. Hydrogen bonds cause the water

molecules leaving the leaf-vessels to pull the molecules in the veins and this upward movement is transmitted along the vein to the roots. To the cohesion is related the surface tension; the rate which describes how difficult is to tense or derange the surface of the liquid. Water has higher surface tension than most other liquids. At the transition between the water and air there appears an exact collocation of water molecules which are bound to the molecules of water underneath. This explains the behaviour of water as it would be covered by an invisible coat; for a biological example high surface tension enables some animals to stand, walk or run on the water surface without disturbance.

2.1.1.2 Hydrological cycle

Existence of the hydrosphere and the water cycle is one of the greatest peculiarities of our planet. Under favourable circumstances and in particular, the combination of size and position of the Earth in the solar system, the atmosphere was created. The water cycle or hydrological cycle is the continuous circulation of water on the surface and in the atmosphere caused by solar energy and gravitational forces. The water cycle is the main subject of hydrological investigation. The start and end of the hydrological cycle is not clearly defined.

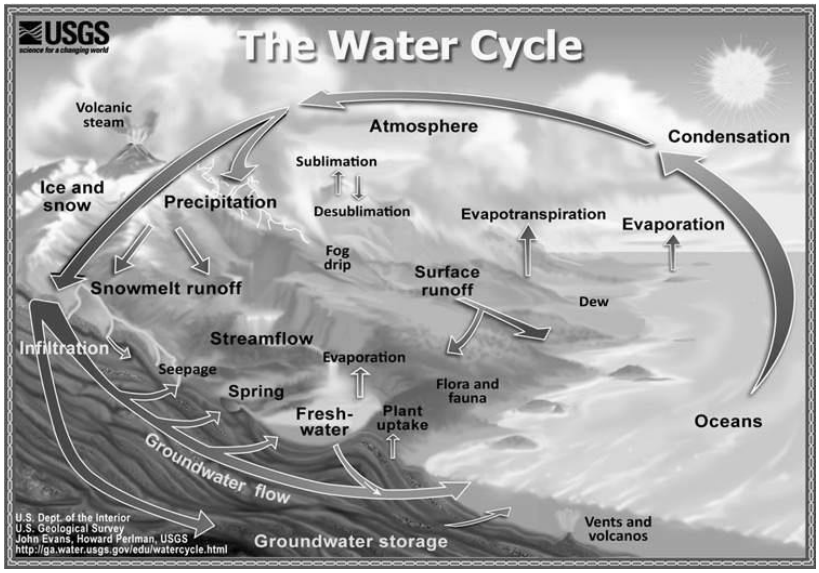

Fig. 2.1 The water cycle scheme from water.usgs.gov

The water cycle includes evaporation, transmission of water vapour, condensation, precipitation and runoff. Small water cycle takes place continuously over the surface of the ocean, and the large water cycle includes the exchange of water between the ocean and land. Water in the form of precipitation reaches the earth's surface due to gravity and

relatively quickly flows into the sea, creeks and rivers. Some of the water percolates into the soil, either welling up to the surface like a spring, which - from the stream - becomes a river and after a certain time reaches the sea, or seeps directly into rivers or the sea. A certain portion persists for a long time in the solid phase as snow and ice, but then melts and flows into the sea. Heat from the sun evaporates water from the sea, rivers and lakes, but also from the soil and plant leaves (transpiration). Water in a gaseous state (water vapour) rises high into the atmosphere, or if it comes into contact with the cold convection, cools down. Cold air accounts for the precipitation or condensation of water vapour, so that air saturated with water condensate into tiny water droplets. These tiny water droplets create clouds (near the ground surface this phenomena is called fog, mist or dew); cohere to each other with even larger droplets and eventually due to its own weight, falls to the ground according to gravity in the form of precipitation. Water molecules move continuously across the hydrosphere by various physical processes and do not necessarily complete all the stages of the cycle.

2.1.2 Heat and temperature

Everything that is in motion has kinetic energy. Atoms and molecules have kinetic energy because they are moving constantly. The faster the molecule moves, the greater is its kinetic energy. Heat is given by the total amount of kinetic energy reflecting molecular motion in the body during heat exchange. When the average molecular motion increases, it is being registered by thermometer as a temperature increase. Heat and temperature are closely connected are not the same thing. Temperature indicates if the body will receive or release the heat whilst contacting other bodies. Whenever two bodies with different temperatures meet, the heat is transferred from the warmer body to the colder body until the temperatures are equal. Molecules of the colder body increase their motion at the expense of kinetic energy of the warmer body.

2.1.2.1 Specific heat capacity of water

Specific heat capacity of a substance is defined as the amount of heat which 1g of this substance has to absorb or release, so its temperature changes about 1 °C. Heat capacity of water is 4186 [$J \cdot kg^{-1} \cdot K^{-1}$]. In comparison with other substances, the specific heat capacity of water is high. This can be explained, as well as many other features, by hydrogen bonds. When the heat is being absorbed, hydrogen bonds are destroyed; when the heat is being released, hydrogen bonds are created. Heat causes relatively small changes in water

temperature, because most of the heat is used for the dissipation of the hydrogen bonds even before the motion of water molecules become faster. While the temperature of water slowly decreases, many new hydrogen bonds are created which leads to the release of significant amount of energy (Campbell & Reece, 2006a).

Water stabilises air temperature by absorbing or releasing the heat to the air. Water works as a temperature bank; it can absorb or release relatively huge amounts of heat with only a little change of its own temperature. This ability originates from its large specific heat capacity (Campbell & Reece, 2006a). During the daytime and in summer in the Northern hemisphere (and winter in the Southern hemisphere), an enormous volume of water can absorb and store big amount of heat coming from the Sun, meanwhile the temperature of water increases only about few degrees. During the night and in winter the gradual cooling of water could warm up the air. This is the reason why in the coastal areas commonly have a milder climate than in the inland regions. High heat capacity has a tendency to preserve the temperature of the oceans, where the suitable conditions for marine life are created (Campbell & Reece, 2006a).

2.1.2.2 Latent heat of vaporization

High latent heat of vaporization (λ) is another feature of water explained by the presence of hydrogen bonds which need to be destroyed before the molecules leave the liquid. Latent heat of evaporation of water also stabilizes the climate on Earth. A significant amount of solar heat, which is being absorbed by the oceans in tropical regions, is consumed to evaporate molecules from the water surface. Then, when the humid tropical air mass moves to the poles, it releases the heat while its condensates and creates precipitation (Campbell & Reece, 2006a). Latent heat of vaporization expresses the energy required to change a unit mass of water from liquid to water vapour in a constant pressure and constant temperature process. The value of the latent heat varies as a function of temperature. At a high temperature, less energy will be required than at lower temperatures. As λ varies only slightly over normal temperature ranges a single value of 2.45 $MJ \cdot kg^{-1}$ is taken in the simplification of the FAO Penman-Monteith equation. This is the latent heat for an air temperature of about 20°C (Allen et al, 1998).

2.1.2.3 Latent heat flux

Flux or water flux is typically expressed as volume per area per unit of time. Flux is used to express the rate at which water permeates a reverse osmosis membrane. Typical units of measurement are litres per square meter per hour [$l \cdot m^{-2} \cdot hr^{-1}$]. The flux of a reverse osmosis membrane is directly proportional to temperature and pressure (ROChemicals, 2013). In meteorology, latent heat flux is the flux of heat from the Earth's surface to the atmosphere which is associated with evaporation or transpiration of water at the surface and subsequent condensation of water vapour in the troposphere. It is an important component of Earth's surface energy budget. Latent heat flux has been commonly measured with the Bowen ratio technique, or more recently since the mid-1900s by the eddy transfer coefficient (eddy covariance method).

2.1.3 Evaporation

Molecules of any liquid stay together by being attracted one to another. Molecules, whose motion is fast enough to exceed this force, are able to abandon the liquid and enter the air as gases. This transformation is called evaporation. Velocity of the molecules varies and temperature is dependent on average kinetic energy of molecules. Even under the low temperatures, the fastest molecules can escape into the air. By warming by the liquid, the kinetic energy of molecules increases as well as the rate of evaporation.

When a liquid evaporates, its surface cools down. This cooling by evaporation occurs because the molecules with the greatest kinetic energy have the highest probability to be transformed into the gas. Evaporation cooling of water contributes to stabilize the water temperature in lakes and ponds and provides the mechanism which prevents overheating of terrestrial fauna (Campbell & Reece, 2006a).

2.1.4 Groundwater and infiltration

Groundwater is part of the Earth’s water cycle that flows underground. Water infiltrates into the ground and follows the path of least resistance through air pockets between soil and rock particles. Water first passes through the zone of aeration or unsaturated zone. From here, water is taken up by plant roots, discharged into a body of water, or flows down to the next zone, which is the zone of saturation or saturated zone. Here all the spaces between the particles are completely filled with water. The top of this zone is called the water table. Infiltration denotes the entry of water into the soil through its

surface, the absorption and downward movement of water into the soil layer and flow of water from the land surface into the subsurface.

2.2 Water transport mechanisms in soil

Soil is a medium for plant growth or bio-materials production whereby this medium combines with the other soil functions to anchor roots, and allow for the transport of water and nutrients to the root/soil interface (NRCAA, 2010).

Usually the energy status of soil water in a particular location in the profile is compared to that of pure water at a standard pressure and temperature, unaffected by the soil and located at some reference elevation. The difference in energy levels between this pure water in the reference state and that of the soil water is called soil water potential (the term potential implies difference in energy status). Soil water potential is due to several forces, each of which is a component of the total soil water potential (Ψt).

Three main types of forces which contribute to the energy state of soil water include: In an unsaturated soil, matric potential resulting from the capillarity and adhesion forces. Plants must overcome the energy of matric potential to extract water from the soil (UBC, 2014).

2.2.1 Soil water movement

The movement and retention of water, uptake and translocation in plants, and loss of water to the atmosphere are controlled by energy gradients. The forms of energy involved are potential (related to position), kinetic (related to movement), and electrical (related to cations and anions). The difference in energy level of water from one site or one condition (wet soil) to another (dry soil) determines the direction and rate of water movement in soils (and in plants) (UBC).

Water flow can take place in saturated and/or unsaturated soils -depending on position of water in flow field and geometry (shape, size, continuity) - of pores.

The rate at which water flows is directly proportional to the water potential gradient, and the proportionality factor is called hydraulic conductivity (*K*). This relationship is described by Darcy's Law:

$$\boldsymbol{q = -K -\left(\frac{dy}{dz}\right)} \quad (1)$$

where q is water flux density - the rate of water flow crossing a plane in unit time. The plane through which water flows is perpendicular to the axis of flow. Water flux is the rate of water flow crossing the plane in $m^3 \cdot s^{-1}$. Flux density is the flux divided by the area of the plane in $m^3 \cdot m^{-2} \cdot s^{-1}$ or $m \cdot s^{-1}$.

2.2.1.1 Hydraulic potential

The potential of water is influenced by binding forces as well as by gravity and external pressure. In unsaturated soil water is bound to the soil matrix in three ways – through water molecules held directly to the solid phase by Van der Waal's forces; by capillary action as a result of adhesive and cohesive forces and by osmotic forces between clay particles and organic matter.

$$\boldsymbol{\Psi_H = \Psi_m + \Psi_g} \quad (2)$$

2.2.1.2 Gravitational potential

Gravitational potential ($+\Psi_g$) is defined as energy required to rise a unit of water from a free water surface (GWS) to a certain height (h) in a soil pore (capillary) against gravity force.

2.2.1.3 Matric potential

Matric potential ($-\Psi_m$) is defined as the energy required to extract a unit of water from a soil pore (capillary) against its capillary force.

2.2.1.4 Osmotic potential

Osmotic potential ($-\Psi_o$) is energy required to extract a unit of clear water through a semipermeable membrane from soil solution.

2.2.1.5 Field capacity

Once infiltration has ceased, water in the largest soil pores will drain downward quite rapidly. After one to three days, this rapid downward movement becomes negligible and matric forces begin to play a greater role in water movement. The soil is then at field capacity. In this condition, water has moved out of macropores and air has moved in. Micropores are still filled with water and continue to supply plants. Drainage continues but is much slower. Field capacity often corresponds to a matric potential of -1 to -3 m (or -10 to -30 kPa), assuming drainage into a less-moist zone of similar porosity (UBC).

2.2.2 Water vapour movement

Water is also able to move through soils as the water vapour, the most important example of this being the loss of water vapour by evaporation from soil surfaces. This occurs when the concentration of water vapour in the soil close to the surface is higher than in the atmosphere immediately above. Water vapour will then move from the soil into the atmosphere in an attempt to equalize concentrations. The drier and hotter the atmosphere compared with the surface soul, the greater will be the rate of evaporation from the soil, provided sufficient water can be supplied to the surface by capillary movement from below (Bot & Benites, 2005).

2.3 Water transport mechanisms in plants

From the evolutionary point of view, algae, predecessors of terrestrial plants, lived in water environment. Therefore each of its cells had water and nutrients at any time available. Evolution brought terrestrial life expansion and diversification of plant body into the root (which pumps the water and minerals from the soil) and shoots (aboveground part exposed to the sunlight and atmospheric CO_2). As a consequence of these morphological changes, plants have the ability to obtain vital substances from air and soil, a new issue appeared: the necessity to transport the substances between the roots and the shoots. Their connection is provided by vascular bundles which transport the sap throughout the plant body (Campbell and Reece, 2006b).

2.3.1 Water potential and its importance for plants

The survival of a plant is dependent on its ability to maintain water intake and output in balance. Water intake and losses on a cellular level occur by osmosis, a passive transport of water through the cellular membrane. Water moves from the hypotonic medium into hypertonic medium. In the case of plant cells, due to the presence of a cell wall, there also has to be taken into account another factor - pressure. By the combination of these two components (concentration of the solution and pressure) we get water potential (greek letter Ψ). This potential is characterised as water always moves from the area with higher Ψ to an area with lower Ψ. Unit of water potential is megapascal (MPa), 1 MPa roughly corresponds to the pressure of 10 atmospheres (atm). (Atm ispressure measured at the sea level created by air mass column above Earth's surface – approximately 1kg 1cm^2).

Water potential can be understood as the force with which water permeates through the membranes of plant cells. Transport through the cell membranes is regulated by aquaporins, membrane proteins. They affect the velocity of water flowing in the gradient direction of water potential. A plant can thereby regulate the velocity of water intake and outflow if its inner water potential differs from the ambient water potential. Aquaporins create selective channels which open and close as a response to, for example, turgor pressure (Campbell & Reece, 2006c).

By the increasing concentration of the solution, the water potential decreases. Molecules of water surround the dissolved molecules of matter. They are less mobile than

molecules of pure water. Unlike the inverse relationship of the Ψ and solution concentration, Ψ directly correlates to pressure - Ψ increases with increasing pressure. If the water and solution are separated by a semipermeable membrane, it is possible to inhibit its feature of osmotic intake of water molecules by external pressure (Campbell & Reece, 2006d).

The combination of the concentration influence of the solution and pressure on water potential is expressed as:

$$\boldsymbol{\Psi = \Psi p + \Psi o} \quad (3)$$

Where Ψ_p is pressure potential (pressure on solution) and Ψ_o, as described in 2.2.1.3, is osmotic potential (proportional to the concentration of a given substance in a solution) (Campbell & Reece, 2006c).

2.3.1.1 Pressure potential

Pressure potential (Ψ_p) is the component of water potential due to the hydrostatic pressure that is exerted on water in a cell. In turgid plant cells it usually has a positive value as the entry of water causes the protoplast to push against the cell wall. In xylem cells there is a negative pressure potential, or tension, as a result of transpiration. Water at atmospheric pressure has a pressure potential of zero (Dictionary of Biology, 2004).

$$\boldsymbol{\Psi p = \frac{P}{\rho_w}} \quad (4)$$

P is pressure and ρ_w is density of water.

2.3.1.2 Transport of water through xylem

Transport of substances in plants takes place at three levels: 1) intake and output of water and solutions by the cells (eg. Intake of soil water by the root cells); 2) short distance

intercellular transport within tissues and organs (eg. transport of saccharides from leaf mesophyle to phloematic net cells); and 3) long distance transport by specialized vascular tissues (xylematic and phloematic) (Campbell & Reece, 2006b).

By xylem, water and minerals (sap) flow upwards through the stem into the leaves to maintain nutrient supply to each cell. Leaves are thereby dependent on the water supply. A plant loses an incredible amount of this liquid by transpiration. Evaporation of water occurs mostly from the leaf surface and other aboveground parts. In case this water loss is not recharged (by water uptake by the root system), leaves wilt and die.

During the night, meanwhile the transpiration occurs only at a small rate or does not occur at all, the energy is spent in root cells to transport the water and ions into the xylem. Endodermis surrounding the stele enables the reverse penetration of ions back into the root bark. Accumulation of ions in stele leads to a decrease of local water potential. As water flows into the stele from the root bark, pressure increases which stimulates the upward movement of the sap to the aboveground plant parts. Guttation (dew creation) is a consequence of the root uplifting forces. Guttation is the excretion of water drops on leaf tips of grasses and leaf edges of small herbaceous dicotyledonous plants. Dew is created during the night, when the transpiration is radically inhibited, when more water gets into the leaves then it is evaporated. This abundant amount of water is pushed out on the leaf surface and creates a water drop (Campbell&Reece, 2006d).

Diffussion is a suitable mechanism for the transport of water on the cellular level, but is too slow for the transport of substances from the roots to the leaves. Transport of water over long distances is provided by mass flow through xylem and phloem. In the case of phloem – liquid is pressed by the hydrostatic pressure from one end of the net cell to another. Motion transport force in xylem is the negative pressure created by water evaporation in the aboveground plant parts, mostly leaves. This process is called transpiration.

2.3.2 Transpiration

Thanks to transpirational flow, the water and minerals are pulled through the root hair from the soil solution up to the leaves. Cohesive forces between water molecules provide

togetherness of the water column moving upward through xylem. The water molecule, which leaves the xylematic cell in the leaf, pulls the adjacent water molecule. This traction is transmitted from molecule to molecule downwards by xylem. Adhesion of water molecules to the hydrophilic cell walls also helps to overcome gravitational force. Transpirational flow upward to the leaves occurs as a consequence of water evaporation from the leaves and by the cohesion of water molecules. The cells of leaf mesophyll are exposed to CO_2 (essential for photosynthesis) due to the presence of the complex system of water chambers (microscopic pores on leaf surface) under the stomata. Air in these chambers is in contact with moist cell walls and thus become saturated by water vapour. Usually, the ambient air is drier (contains lower amount of water vapour) than the air inside the leaves. Water vapour leaves the leaf by the stomata openings while being in the direction of its concentration gradient.

Water vapour released from the cellular spaces in leaves by transpiration is being constantly replaced by evaporation from thin layers of water covering the walls of these cellular spaces. After the water is evaporated, the remaining water layer is sucked into the pores of the walls (in consequence of adhesion to hydrophilic cell walls). At the same moment, the cohesive forces among the molecules (water surface potential) preclude the possibility of enlargement of the hydro layer. Thereby water is pulled upwards through xylem by adhesive and cohesive forces. Due to these features, adhesion of water to the cell walls and high water surface potential, the meniscus (a bulge of water surface) is created. Logically, the more negative pressure acts on the hydro layer (this pressure is smaller than the atmospheric one), the more concave is the meniscus. Negative pressure (a tension) of the hydro layer surface covering the air spaces in leaves is a physical prerequisite for transpirational flow which pulls water upwards trough xylem.

2.3.2.1 Regulation of transpiration

Transpirational flow prevents wilting, supplies leaves with water and participates in mineral and nutrient transport from the roots to the stem and leaves. By evaporation, leaves are cooled by 10-15 ℃ in comparison to the ambient atmosphere. This ability protects the leaf against reaching such temperatures which may cause inter alia denaturing of most photosynthetic enzymes. If the transpiration exceeds the water supply by xylem, the soil

dries, leaf cells lose their turgor and wilt. However, plants are not helpless against impacts of the external environment. They are able to adapt. Equilibrium is reached by photosynthetically-transpirational compromise, a mechanism which regulates the size of the stomatal openings (Campbell & Reece, 2006d)

A plant does not consume anything from its metabolic energy to create transpirational flow (Campbell & Reece, 2006d). In brief, it is the sunlight that is responsible for evaporation of water from the wet chamber walls in leaf mesophyll (inner spaces are thereby permanently saturated with water vapour). Upward flow of water through xylem is powered by solar energy (Campbell & Reece, 2006d).

The light can stimulate stomatal opening. This can happen due to photosynthesis control in chloroplasts of clamp cells, where the ATP available for active transport of hydrogen ions is synthesized. The second incentive for stomatal opening is depletion of CO_2 storage in sponge parenchyma of the leaf, which occurs during photosynthesis initiation in mesophyll. The third method of regulation is the internal clock of stomata. Even if the plant would be placed into a dark cabinet, the stomata would continue its daily rhythm of closing an opening. All eukaryotic organisms have this inner clock which track time and regulate cyclic processes (Campbell & Reece, 2006d). These cycles with cca 24 hour intervals are termed circadian rhythms.

2.3.3 Photosynthesis of C4 plants

One of the possibilities how to assess the efficiency of water use by plant is to determine the ratio between the photosynthesis and evaporation (Campbell & Reece, 2006, p.759). In many plant species this ratio is 600:1 (the amount of water consumed to convert 1 g of CO_2 into organic compounds during photosynthesis). Notwithstanding, corn and other plants which assimilate atmospheric CO_2 by C4 cycle (Hatch and Slack pathway), have a ratio of evaporation and photosynthesis 300:1, or even less. Photosynthetic gain for every 1 gram of water is higher in C4 plants; even under the same concentration of CO_2 in intercellular spaces of leaf (Campbell & Reece, 2006d).

2.3.3.1 Leaf morphology and principle of C4-photosynthesis

The unique morphology of the leaf corresponds with the processes of C4-photosynthesis. Composition and biochemical processes in leaves of C4-plants are an evolutionary adaptation to hot and dry climate (Campbell & Reece, 2006e).

Two different kinds of photosynthetic cells are present in C4-plants: bundle-sheath cells and mesophyll. Sheath cells are organized into tightly adjacent sheaths around the vessels in the leaf. Between the bundle-sheath and leaf surface, there are, more freely placed, mesophyllic cells. The Calvin cycle is limited only to chloroplasts in the bundle-sheath. C4 plants can assimilate CO_2 in higher rate and faster than the C3 plants, because the water loss allows CO_2 enter into the leaf. In C4-plants, the carbon is incorporated different way. At first, CO_2 is connected to PEP (phosphoenolpyruvate) and compound oxalacetate is created. This compound with four atoms of carbon in molecule is the origin of the name C4. The enzyme which connects CO_2 to PEP is called PEP-carboxylase. In comparison with RuBPcarboxylase (present in C3 cycle), PEP-carboxylase has very high bonding affinity for CO_2. This is the reason why the CO_2 can be fixed by C4 plants sufficiently, even when the RuBPcarboxylase is not able – under the hot and dry conditions while stomata are partially closed, which leads to a decrease of CO_2 in the leaf and concentration of O_2 increase.

The C4 pathway is being used by a few thousands plant species in at least 19 plant families (Campbell & Reece, 2006e). Among the C4 plants important for the agricultural production, there are, inter alia, members of family *Poaceae* (grasses) - sugar cane, and corn.

2.4 Corn crop (Zea Mays)

Maize or Corn plant (e.g. *Zea Mays*) species belongs to the kingdom plants (*Plantae*), division flowering plants (*Magnoliophyta*), class monocotyledons (*Liliopsida*), order *Poales*, family *Poaceae* (also called *Gramineae* or true grasses).

Domestication of corn from the wild grass lies at the foundation of sedentary living and civilization in central America 7000 years ago. Cultivated corn is known to have existed in the SW USA for at least 3000 years. To the Aztecs and the Incas, corn was a

staple of their diet. The necessity to produce, preserve and process food led to many technical inventions. During the 16-17th centuries, after Christopher Columbus, Genoese sailor and coloniser, laid the foundation stone of business traditions. These traditions formed the basis of the world's food structure as we know it today. Indian corn (corn, maize) ranks third behind rice and wheat in total world production.

2.4.1 Corn development and growth

The success of the modern corn producer depends on making good decisions regarding production and management practices. Any management practice that the grower can better manage or optimize will increase the profitability or returns after costs. This margin is important for continued financial sustainability of corn producers.

Management decisions are optimized for various growth stages. Growth stages are divided into vegetative and reproductive. The vegetative stages begin when the seedling emerges and continues until the tasseling, when reproductive stages begin. During the vegetative stage, leaves and roots develop and grow, the stalk forms, and reproductive structures (ear and tassel) begin to form. The reproductive stages begin with pollination and end when grain development is complete. In the Northern hemisphere the reproductive stages begin in early to mid-July and end about mid-September (Smith et al, 2004).

2.4.2 Corn biomass production and light interception

Grain yield is the proportion of biomass produced by the plant that is harvested at maturity (Smith et al, 2004). This proportion, usually referred to as harvest index (HI), is very stable when water and nutrients do not limit growth (Sinclair et al., 1990; Otegui et al., 1995). This stability highlights the importance of biomass production during the growing season to obtain maximum grain yield (Smith et al, 2004).

Crop biomass is the final balance between two processes: CO_2 gain through photosynthesis and CO_2 loss due to respiration. Because the ratio between loss and gain is relatively constant, and the former depends directly on light interception by the canopy, any increment in photosynthetically active radiation (PHAR, range of solar radiation within the 400-700nm wavelengths; more about PhAR in the chapter 3.2.13) intercepted by the crop

should promote a proportional increase in growth (Monteith, 1977; Gallagher and Biscoe, 1978). Shoots biomass production can be expressed as the product of incident PhAR (IPAR), the capacity of the canopy for intercepting IPAR (e_i efficiency of interception), and the efficiency of the crop for converting intercepted IPAR ($IPAR_i$) into biomass (*RUE*, radiation use efficiency) according to shoots biomass at day:

$$N = \sum_{0}^{N} IPAR_i \cdot e_i \cdot RUE \quad (5)$$

The time considered for computing shoots biomass, *N*, can correspond to the entire growing season or a period within it. Local environment conditions set an upper limit on N (e.g. low temperatures early and late during the growing season) and thus to the maturity group that can be used at a given location. The amount of IPAR is also site-specific and varies markedly with the latitude and the day of the year (e.g. maximum at the summer solstice) (Smith et al, 2004).

The quality and composition of corn for processing is greatly affected by environmental conditions and genetics (Rooney & Suhendro, 2011). The fibre and ash are concentrated in the pericarp. The germ contains higher levels of oil and protein. The endosperm contains all the starch and 70% more of the total protein. The type of carbohydrate in the endosperm and the proportion of endosperm to germ affect corn composition (Smith, et al 2004).

2.4.2.1 Corn products: starch, proteins, lipids and other important compounds

Starch in the form of simple spherical granules (diameter from 2 to > 20 micrometer) is the major product of the corn wet-milling industry. Starch granules are used as an ingredient, modified (chemically, enzymatically, or physically), or further processed into glucose and fructose or other industrial chemicals. Modified waxy starches are widely used in the food industry. Waxy starch gels do not undergo retrogradation or syneresis as readily as do gels from normal conrnstarch. The amylose content of cornstarch is 20 to 30 % with an amylopectin content of 70 to 80%. (Amylopectin is the high-molecular-weight glucose polymer, which gives the granule its basic composition; amylose is a lower-molecular-weight polymer with only α-1.4 linkages.)

Corn proteins are classed into four groups: albumin, globulin, prolamin (zein), and glutelins. Corn, sorghum, and millet proteins are significantly more difficult to extract than the proteins of wheat, barley, rye and oats. This has led to modified extraction processes using beta-mercaptoethanol and detergent to improve the extraction to 90% or higher recovery of the protein in the corn. The amino acid content of corn is similar to that of the other cereals in that it has reduced levels of lysine and tryptophan and large quantities of proline, glutamic acid, and other nonessential amino acids. The germ proteins of corn have excellent protein quality with good quantities of lysine and tryptophan.

Corn contains 4% ether extract which is composed primarily of triglycerides that are high in oleic and linoleic acid. Corn is sometimes considered an oilseed since large quantities of corn germ are produced as a co-product of wet and dry milling. (The germ of wet-milled corn contains 40 to 50% oil; dry-milled germ is significantly lower because there is no solubilisation of protein and other components during dry milling. Thus, the residue of dry-milled germ has significantly higher protein content and quality than that of wet-milled germ. Corn oil has excellent properties for kitchen use and is often used in frying of corn snacks.

Corn contains significant levels of phytin, vitamins, and phenolic compounds that are concentrated in the germ, aleurone layer, and peripheral endosperm area. Phytic acid forms pthytin which complexes with calcium, iron and other cations. Phytases are not present in monogastric animal digestive systems, so phytin is excreted into the feces. High-phytase corns have been developed to improve the utilization of minerals by livestock and to reduce the level of phosphorus and calcium present in wastewater from livestock feeding operations (Smith et al, 2004).

3 Goals and outline

The main aim of the work is to compare methods available for the crop water consumption – sap flow, which has the plant physiological approach and the BREB technique with its micrometeorological approach, used to measure transpiration and actual evapotranspiration of maize crop.

The first goal of the investigation thus became trying to find out if the comparison of total evapotranspiration measured by the BREB method and transpiration measured by sap flow technique would lead to the estimation of the evaporation. As a second goal, it therefore became necessary to clarify whether it is possible to deduce the canopy water supply from the comparison of BREB and sap flow and if a time shift of both phenomena exists. It appeared reasonable to set a third goal – to attempt to find out if the mentioned method would be useful in assessing the water balance of the site.

Evapotranspiration is affected by various factors like weather parameters (radiation, air temperature, humidity and wind speed etc.) which are described in next chapters. Crop characteristics – crop type, variety (chapter 2.4 is dedicated to the crop type) and development stage – (crop height, crop roughness, reflection, ground cover and crop rooting), plant density also influences evapotranspiration. This work I focused on the topic of evapotranspiration from the weather parameters approach. Management and environmental aspects like soil salinity, fertility, presence of hard and impermeable soil horizons, diseases and pests control are equally important characteristics, but their inclusion in the experiment would be outside the scope of this work. Chapter 4 describes the used materials and methods, detailed description of the applied equations, principles of data collecting and data processing. Results are presented in chapter 5. A discussion is provided in chapter 6 and the conclusions are drawn in chapter 7.

4 Materials and Methods

The actual evapotranspiration was measured by BREB method, transpiration by sap flow technique, both developed by EMS Brno, Czech Republic. Other environmental factors as e.g. precipitation, throughfall of water in crop, aerodynamic characteristics above crop canopy etc., were measured simultaneously. The difference between both measured phenomenas gives us the idea of the passive water flow through the maize agroecosystem in optimal case. It should serve well for the understanding of the maize crop water balance.

4.1 Experimental setup

1st activity: Installation of the sap-flow sensors. Term: April – June 2013. Locality: Červený Újezd, Velvary, campus of the CULS. 2nd activity: Verification of the data set. Term: November 2013. 3rd activity: Data processing and comparison with other results. Term: February 2014. 4th activity: Final work, elaboration of answers to the opponent reviews.

4.1.1 Location and Canopy parameters

The measurements of actual evapotranspiration was carried out during the period May-September 2013 in the locality Budihostice (Sazená airport) - CULS experimental site - Central Bohemia; 50°19’7.23"N, 14°15’42.371"E, 233 m a.s.l. Soil type of the site is the Haplic Chernozem. A well structured Chernozem has a ratio Matrix/Water/Air 50:30:20 (Rampazzo, 2013, pers. comm.). Technical telecommunications are carried out by Data GSM modul Cinterion TC65 – Terminal; Type of the control panel is Datalogger EdgeBox V8 (both EMS Brno, CZ).

For the experiment, the corn field (*Zea Mays L.*) had been chosen. The corn was sown into 75 cm wide rows on April 19, 2013.

4.2 Model equations and data collecting

In this chapter, the methods are explained while the emphasis is put on the description of the used equations and auxiliary formulas for better understanding and transparency of the observed phenomena. Most of the formulas and equations and their

derivations are taken from Allen et al. (1998), the guidelines to calculate the reference crop evapotranspiration, developed and published in the FAO Irrigation and Drainage Paper No.24 “Crop water requirements”..

4.2.1 Evapotranspiration

Evapotranspiration consists of two processes: transpiration – water output by a plant by evaporating from its leaf surface and evaporation of water from the soil. According to Hatfield (1990), the evapotranspiration obtaining methods range from the direct measurement techniques using lysimeters to energy balance measurements based on Bowen-ratio, flux profile and eddy-correlation techniques.

4.2.2 Air humidity

Air humidity was measured with Air humidity sensor EMS 33.

$$\boldsymbol{RH = 100\frac{e_a}{e^{\circ}(T)}} \tag{6}$$

The relative humidity (*RH*) expresses the degree of saturation of the air as a ratio of the actual vapour pressure (e_a) to the saturation vapour pressure (e°) at the same temperature (T).

4.2.3 Air temperature

The solar radiation particularly absorbed by the atmosphere and mainly emitted as the heat by the Earth increase the air temperature. The sensible heat of the surrounding air transfers energy to the crop and exerts as such a controlling influence on the rate of evapotranspiration. In sunny, warm weather the loss of water by evapotranspiration is greater than in cloudy and cool weather.

$$\boldsymbol{T_{mean} = \frac{T_{max} - T_{min}}{2}} \tag{7}$$

T_{mean} [°C] for 24-hour periods is defined as the mean of the daily maximum (T_{max}) and minimum (T_{min}) temperatures. It is dimensionless and is commonly given as a percentage. Air temperature was measured by the Air thermometer EMS 31 (EMS Brno, CZ).

4.2.4 Bowen Ratio energy balance

The partition of energy at the surface between sensible heat flux and latent heat flux was formulated by Bowen (1926) and it is obtained by Bowen ratio-energy balance method (Perez et al., 1999; Kustas et al., 1996) by

$$\boldsymbol{\beta = H/\lambda E} \tag{8}$$

H is sensible heat flux and λE is latent heat flux. The Bowen ratio combined with the surface energy balance equation is:

$$\boldsymbol{\lambda E = \frac{R_n - G}{1 + \beta}} \tag{9}$$

$$\boldsymbol{H = \frac{\beta}{(1 + \beta)}(R_n - G)} \tag{10}$$

R_n is the net radiation, G is surface soil heat flux. Empirical relationships between fluxes for an averaging period (20 – 60 min) can be formulated as follows:

$$\boldsymbol{\lambda E = -\frac{\rho_a c_p}{\gamma} K_w \frac{\delta e}{\delta z}} \tag{11}$$

$$\boldsymbol{H = \rho_a c_p K_h \frac{\delta T}{\delta z}} \tag{12}$$

ρ_a is the mean air density [kg·m^{-3}] at a constant pressure, c_p is the air heat capacity, K_w is eddy transfer coefficient for water vapour [m^2·s^{-1}], K_h is eddy transfer coefficient for sensible heat [m^2·s^{-1}], δe is the difference of water pressure assuming $K_h = K_w$ (Reynold's

analogy), δz is difference of heights of the measurements, δT is temperature difference. The BREB method is based on the precondition of the coefficients of the apparent and latent heat being equal, when it is possible to determine the ratio of the sensible and latent heats by measuring the gradients of the air temperature and humidity over the evaporating surface (Pivec & Brant, 2008; Woodward & Sheehy 1983).

$$\boldsymbol{\beta \approx \gamma \frac{T_2 - T_1}{e_2 - e_1}} \tag{13}$$

γ is psychrometric constant, T is temperature and e is water vapour pressure, farther (index 1) and closer (index 2) to the crop canopy.

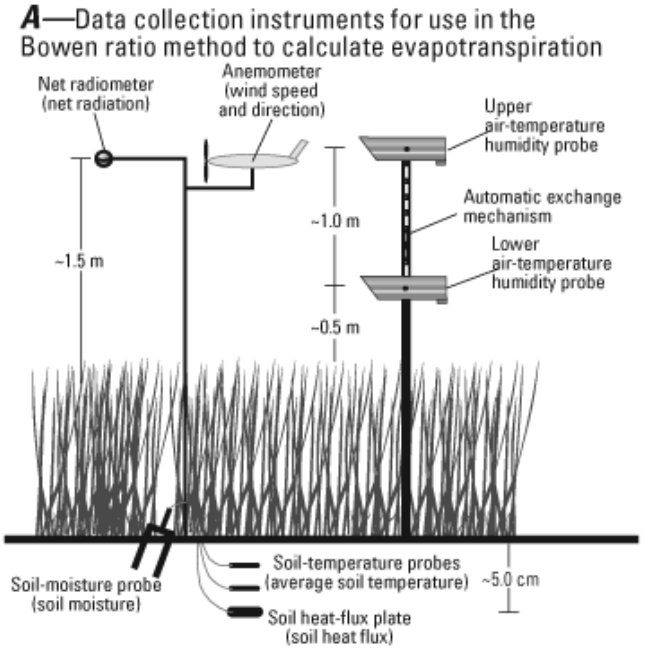

Fig. 4.1.: Scheme of Bowen ratio data collection instruments (pubs.usgs.gov).

Determination of Bowen-ratio measurements of latent and sensible heat fluxes is more involved than for eddy-correlation measurements, because Bowen-ratio sensors are located at two heights (Stannard, 1996), as we can see in the Fig.4.1, rather than just one. Bowen ratio sensor in the field is shown in the Photo 4.1.

4.2.5 Global radiation

Radiation is energy that comes from oscillating magnetic and electric fields and, unlike the other transfer mechanisms, can transfer through empty space. Good examples are the energy one feels from sunlight or from standing near a fire. Radiation that is intercepted by a surface is commonly expressed in terms of energy per unit time per unit surface area (e.g. $W \cdot m^{-2}$). Global radiation or solar radiation is the largest energy source and is able to change large quantities of liquid water into water vapour. The potential amount of radiation that can reach the evaporating surface is determined by its location and time of the year. Due to differences in the position of the sun, the potential radiation differs at various latitudes and in different seasons. The actual solar radiation reaching the evaporating surface depends on the turbidity of the atmosphere and the presence of clouds which reflect and absorb major parts of the radiation (Allen et al, 1998). While assessing the effect of solar radiation on evapotranspiration, one should also bear in mind that not all available energy is used to vaporize water. Part of the solar energy is used to heat up the atmosphere and the soil profile.

$$\boldsymbol{S_t = S_b + S_d = \sin \alpha + S_d} \qquad (14)$$

S_b is the energy of direct beams of the shortwave (sw) irradiance from the Sun. It highly depends on the Sun's position during the day and α is the solar elevation angle. S_d represents the diffuse part of the sw radiation. When dealing with plant communities, it is more accurate to use the following equation considering the new factors while integrating them with the direct and the total irradiation adjusted to the plant vegetation.

$$\boldsymbol{S_{tp} = S_{bp} + S_{dp} + S_{bc} + S_{dc}} \qquad (15)$$

S_{bc} is scattering irradiance on the leaf surface, S_{dc} is scattering irradiance on the ground. Global radiation [$MJ \cdot h^{-1}$, $MJ \cdot m^{-2} \cdot day^{-1}$] was measured with Pyranometer EM11 (EMS Brno, CZ).

4.2.6 Net Radiation balance

Net radiation (R_n) is the amount of radiant energy that is retained by the surface (i.e. the sum of all gains and losses of radiation to and from the surface). *Rn* supplies energy that

heats the air, plants and soil or evaporates water. Net radiation is equal to the sum of its components and the sign indicates whether the radiation is downward (positive) or upward (negative). If the sum of the component parts is positive, as happens during the daytime, then Rn is positive and more energy from radiation is gained than lost from the surface. If the sum of the component parts is negative, as happens during the night, then *Rn* is negative and more radiation energy is lost than gained. (FAO guidelines)

The radiation exchange between atmosphere and a stand (crop canopy) can be determined as:

$$\boldsymbol{R_n = S_{tp} - S_{tr} + L_d - L_u = S_{tp}(1 - \rho_{rt}) + L_n} \quad (16)$$

R_n is net radiation flux [W·m^{-2}], S_t is total radiation in a stand, S_{tr} is the total reflected radiation, L_d is the downward longwave (lw) radiation, L_u is the upward lw radiation, L_n is total lw irradiance on the lower surface, and ρ_{rt} is a reflection coefficient. Net radiation balance was measured with Net radiometer 8110.

4.2.7 Penman-Monteith equation

$$\boldsymbol{\lambda ET = \frac{\Delta(R_n - G) + \rho_a c_p \frac{(e_s - e_a)}{r_a}}{\Delta + \gamma\left(1 + \frac{r_s}{r_a}\right)}} \quad (17)$$

Where R_n is the net radiation, G is the soil heat flux**,** (e_s – e_a) represents the vapour pressure deficit of the air, ρ_a is the mean air density at constant pressure, *cp* is the specific heat of the air, Δ represents the slope of the saturation vapour pressure temperature relationship, γ is the psychrometric constant, and r_s and r_a are the (bulk) surface and aerodynamic resistances respectively.

4.2.7.1 Aerodynamic resistance

The transfer of heat and water vapour from the evaporating surface into the air above the canopy is determined by the aerodynamic resistance:

$$\boldsymbol{r_a = \frac{\ln\left[\frac{z_m - d}{z_{om}}\right]\ln\left[\frac{z_h - d}{z_{oh}}\right]}{k^2 u_z}} \quad (18)$$

Where: r_a aerodynamic resistance [s m^{-1}], z_m height of wind measurements [m], z_h height of humidity measurements [m], d zero plane displacement height [m], z_{om} roughness length governing momentum transfer [m], z_{oh} roughness length governing transfer of heat and vapour [m], k von Karman's constant, 0.41 [-], u_z wind speed at height z [m s^{-1}].

4.2.7.2 Bulk (surface) resistance

According to Allen et al. 1998, the 'bulk' surface resistance describes the resistance of vapour flow through the transpiring crop and evaporating soil surface. Where the vegetation does not completely cover the soil, the resistance factor should indeed include the effects of the evaporation from the soil surface. If the crop is not transpiring at a potential rate, the resistance depends also on the water status of the vegetation. An acceptable approximation to a much more complex relation of the surface resistance of dense full cover vegetation is:

$$\boldsymbol{r_s = \frac{r_l}{LAI_{active}}} \tag{19}$$

Where: r_s (bulk) surface resistance [s·m^{-1}], r_l bulk stomatal resistance of the well-illuminated leaf [s·m^{-1}], LAI_{active} active (sunlit) leaf area index [m^2 (leaf area) m^{-2} (soil surface)].

4.2.7.3 Leaf Area Index (LAI)

Leaf area index, the main determinant of light interception depends on the area of the leaves and the rates of leaf appearance and leaf expansion. The *LAI* values for various crops differ widely, but values of 3-5 are common for many mature crops (Allen et al. 1998). *LAI* changes throughout the season and normally reaches its maximum before or at flowering. *LAI* further depends on the plant density and the crop variety. LAI_{active} (sunlit) leaf area index is given in [m^2 (leaf area) m^{-2} (soil surface)].

$$\boldsymbol{LAI_{active} = 0,5LAI} \tag{20}$$

The fact that generally only the upper half of dense clipped grass is actively contributing to the surface heat and vapour transfer is taken into consideration in this equation. For clipped grass a general equation (where *h* is crop height) for LAI is:

$$\boldsymbol{LAI = 24 \cdot h} \tag{21}$$

4.2.7.4 FAO Penman-Monteith equation

The modified Penman method was considered to offer the best results with minimum possible error in relation to the living grass reference crop (Allen et al. 1998). From the original Penman-Monteith equation and the equations of the aerodynamic and surface resistance, the FAO Penman-Monteith method to estimate ET_o can be derived:

$$\boldsymbol{ET_O = \frac{0.408\Delta(R_n - G) + \gamma \frac{900}{T + 273} u_2 (e_s - e_a)}{\Delta + \gamma(1 + 0.34u_2)}} \tag{22}$$

where ET_o is reference evapotranspiration [mm day^{-1}], R_n is net radiation at the crop surface [MJ m^{-2} day^{-1}], G is soil heat flux density [MJ m^{-2} day^{-1}], T is mean daily air temperature at 2 m height [°C], u_2 is wind speed at 2 m height [m s^{-1}], $(\boldsymbol{e_s - e_a})$ is saturation vapour pressure deficit [kPa], Δ is slope of saturated vapour pressure curve at given temperature [kPa °C^{-1}], and γ is psychrometric constant [kPa °C^{-1}].

4.2.8 Potential evapotranspiration

Potential evapotranspiration (PET) of a given crop is defined as soil evaporation and plant transpiration under unlimited soil water supply and actual meteorological conditions (Labedzki, et al 2011). The potential evapotranspiration is a maximum intensity of evapotranspiration from a large surface covered completely and homogenously with actively growing plants under conditions of unlimited availability of soil water (Brutsaert, 1982). PET can be calculated either for the single leaf or for the entire canopy. The following equation considers the leaf energy budget as a wet system while its temperature is equal to its operative humid temperature:

$$R_{abs} - L_{oe} - H - \lambda E = R_{abs} - \varepsilon_s \sigma {T_L}^4 - c_p g_{Ha}(T_L - T_a) - \lambda g_v \frac{e_s(TL) - e_a}{p_a} \quad (23)$$

R_{abs} is the absorbed radiation, L_{oe} is the emitted thermal radiation, H is the sensible heat loss, λE is the latent heat loss, T_L is the leaf temperature, T_a is the air temperature, g_{Ha} is the heat conductance (1,4·0,135$\sqrt{u/d}$, where u is the wind speed and d the dimension of the leaf), g_v is the vapour conductance for the whole leaf, e_s is the saturation vapour pressure of water depending on temperature, e_a is the air vapour pressure and p_a is the atmospheric pressure.

Penman linearization:

$$\begin{aligned} \lambda g_v \frac{e_s(T_L) - e_a}{p_a} &= \lambda g_v \frac{e_v(T_L) - e_s(T_a)}{p_a} + \lambda g_v \frac{e_s(T_a) - e_a}{p_a} \\ &\approx \lambda g_v s(TL - T_a) + \lambda g_v \frac{D}{p_a} \end{aligned} \quad (24)$$

where D is the vapour pressure deficit of the atmosphere.

$$T_L - T_a = \frac{\gamma^*}{s + \gamma^*} \left[\frac{R_{abs} - \varepsilon_s \sigma {T_a}^4}{c_p g_{Hr}} - \frac{D}{\lambda^* p_a} \right] \quad (25)$$

..

$$\lambda E_{leaf} = \frac{s\left(R_{abs} - \varepsilon_s \sigma {T_a}^4\right) + \gamma^* \lambda g_v D / p_a}{s + \gamma^*} \quad (26)$$

where $\gamma^* = c_p g_{Hr} / \lambda g_v$.

$$H = -k \frac{dT}{dz} \quad (27)$$

where k is thermal conductivity [$Wm^{-1}C^{-1}$], T is the temperature in Kelvin and z is the height (depth) of the soil. To estimate the evapotranspiration from the plant communities, the Penman-Monteith equation (developed by Monteith in 1965) is used:

$$\lambda E_{leaf} = \frac{s\left(R_{abs} - \varepsilon_s \sigma {T_a}^4 - G\right) + \gamma^* \lambda g_v D / p_a}{s + \gamma^*} \quad (28)$$

4.2.9 Precipitation

Atmospheric precipitation is composed from particles which originate by condensation of vapour in air, and which fall down from clouds or deposit on Earth's surface or objects in the atmosphere. Precipitation occurs in liquid or solid phase or mixed. Precipitation can be divided by its origin. Falling precipitation – vertical precipitation - has its origin in clouds. Deposited precipitation – has its origin outside the clouds – (dew, precipitation deposited from fog, white frost, rime, glaze). Precipitation is measured usually by a rain gauge with a tipping bucket. In our experiment, precipitation was measured with SR 03 raingauge - 500 cm^2 by Meteoservis v.o.s, CZ.

4.2.10 Sap flow

Sap flow measurement techniques are used to continuously monitor whole plant physiology. The water flow in a stem – sap flow – just like the water output of the whole plant stand, depends primarily on the evaporation demands of the adjacent layer of the atmosphere, which are represented by e.g. the vapour pressure deficit and also by the input of energy given e.g. by the global solar radiation energy (Pivec 2009, Woodward and Sheehy, 1983).

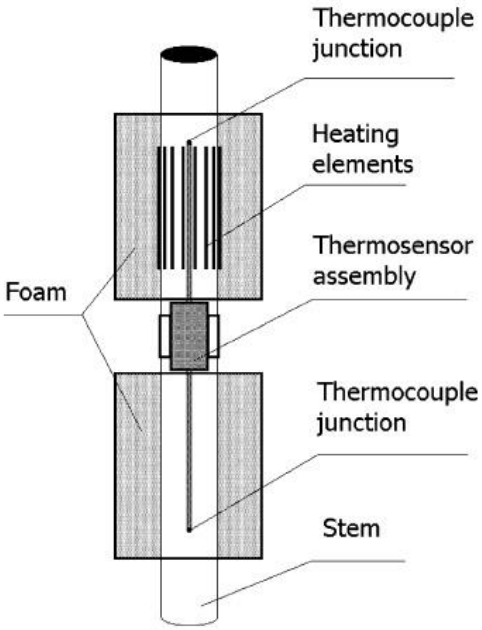

Fig. 4.2: Diagram of the EMS "baby sensor" for shoots or small stems (adapted from Čermák et al. 2004).

Sap flow meter is represented by schematic sketch (Fig 4.2). Thermocouple is inserted into the stem. Thermocouple consists from thermosensor which is placed between two cylinders which are the heating element in the upper part and the isolation element in the lower part. Flow through the stem occurs from the lower into upper part. Information is passed between probes through the connecting wires and passes the information of the temperature differences into the data logger. The magnitude depends on the used metal.

Darcy's law within a plant sap postulates, that the sap is moved by the water potential differences through the xylem elements which put a certain degree of resistance to this movement.

$$\boldsymbol{S = \frac{\Delta \Psi}{R}} \tag{29}$$

$$\boldsymbol{P = Q \cdot dT \cdot c_w + \Delta T \cdot z} \tag{30}$$

where P is the heat input power [W], Q is the sap-flow rate [kg·s^{-1}], ΔT is the temperature difference in the measuring point [K], c_w is the specific heat of water, z is the coefficient of heat losses from the measuring point [W·K^{-1}].

The relationship between the output voltage of a thermocouple and the temperature difference is nonlinear and it is approximated by:

$$\boldsymbol{T = \sum_{n=0}^{N} a_n v^n} \tag{31}$$

The coefficients a_n are given for n from zero to between five and thirteen, v^n is the otput voltage.

The sap-flow Q [kg·s^{-1}] values are derived from following equation:

$$\boldsymbol{Q = \frac{P}{c_w \Delta T} - \frac{z}{c_w}} \tag{32}$$

The magnitude of the heat losses from the sensor can be estimated from the data recorded under the zero evaporating demands as at night before the sunrise or during the rain. Sap flow was measured on 12 plants with the Sap Flow Meter T4.2. The sap flow sensor (Photo 8.2) was installed on 12 plants on 12.7.2013. De-installation of sap flow sensor was 29.8.2013 (1.8.2013). The output from the sensors provided the values in kilograms per hour. To be able to compare the sap flow with the BREB, it was necessary to multiply the values by the number of plants per meter squared which, according to the Brant (2013) site biometrics, is 8.9 (Brant). After this extrapolation from the plant to the whole canopy, the amount of sap flow per m^2 was obtained.

4.2.11 Soil heat flux and soil temperature

According to energy balance validity, the energy arriving at the surface must equal the energy leaving the surface for the same time period. The equation for evaporating surface is written as:

$$\boldsymbol{R_n - G - \lambda\, ET - H = 0} \tag{33}$$

Where *Rn* is net radiation, *H* is sensible heat, *G* the soil heat flux and $\lambda\, ET$ the latent heat flux. All fluxes of energy should be considered when deriving this energy balance equation (Allen, et al, 1998). The values of heat fluxes between the soil layers are calculated according to Fourier's law for the heat transport:

$$\boldsymbol{G = -k\frac{\Delta T}{\Delta z}} \tag{34}$$

G [$W \cdot m^{-2}$] is the heat flux density of the soil, *k* [$W \cdot m^{-1} \cdot K^{-1}$] is thermal conductivity, and $\Delta T/\Delta z$ is temperature gradient. Following equation is based on the idea that the soil heat flux follows soil temperature.

$$\boldsymbol{G = c_s\frac{T_i - T_{i-1}}{\Delta t}\Delta z} \tag{35}$$

G is represented in [$MJ \cdot m^2 \cdot day$], c_s is the soil heat capacity [$MJ \cdot m^3 \cdot °C$], T_i is the air temperature at time i [°C], Ti_{-1} is air temperature at time i-1 [°C], Δt is the length of the time interval and Δz is the effective soil depth [m]. This equation is the correction of the FAO guidelines equation nr. 41. When similar temperatures in day 1 and day 2 are assumed, the FAO equation nr. 42 suggest that for short time intervals, *G* equals to zero. *G* can only be zero if the average temperatures are substracted, not added.

Soil heat flux was measured by Soil heat flux sensor HFP01 (Hukseflux, NL). Soil temperature was measured by the Sensor Pt100/8 (EMS Brno, CZ). Soil temperature was measured at the three depths – 10, 20 and 30cm below ground surface.

4.2.12 Soil water potential and volumetric water content

Soil water potential [kPa] was measured by Watermark 200SS sensors (IRROMETER Company, Riverside, CA), volumetric water content by Decagon EC-10 sensor (Decagon Devices, Inc., USA) [$cm^3 \cdot cm^{-3}$]. Soil water potential determines whether or not a plant is capable of taking up water, regardless of the water content.

4.2.13 Vapour pressure deficit

The difference between the saturation and actual vapour pressure is called the vapour pressure deficit or saturation deficit and is an accurate indicator of the actual evaporative capacity of the air.

Water vapour is a gas and its pressure contributes to the total atmospheric pressure. The amount of water in the air is related directly to the partial pressure exerted by the water vapour in the air and is therefore a direct measure of the air water content. In standard S. I. units, pressure is expressed in pascal (Pa). As a pascal refers to a relatively small force (1 newton) applied on a relatively large surface (1 m^2), multiples of the basic unit are often used. Vapour pressure is expressed in kilopascals (kPa = 1000 Pa).

When air is enclosed above an evaporating water surface, equilibrium is reached between the water molecules escaping and returning to the water reservoir. At that moment, the air is said to be saturated since it cannot store any extra water molecules. The corresponding pressure is called the saturation vapour pressure (e°(T)). The number of water molecules that can be stored in the air depends on the temperature (T). The higher is the air temperature, the higher the storage capacity, the higher is its saturation vapour pressure. The actual vapour pressure (e_a) is the vapour pressure exerted by the water in the air. When the air is not saturated, the actual vapour pressure will be lower than the saturation vapour pressure. The actual air humidity can be calculated as following:

$$\chi = \frac{\mathbf{217}\boldsymbol{e}}{\boldsymbol{T}} \tag{36}$$

χ is the absolute humidity or vapour density [g m^{-3}] (the mass of water vapour in unit volume of moist air), while *e* is the vapour pressure in mbar, T is temperature in Kelvin and ideal gas equation is applied.

4.2.14 Wind direction and wind speed

Wind direction and wind speed was detected by Wind sensor Met One 034B (MetOne Instruments, USA).

Wind is a horizontal transport of the air masses. It can be expressed by a vector and it is characterized by velocity and direction. Horizontal part is consequence of pressure gradient and Coriolis force (force of deflecting Earth's rotation). Vertical part is result of air motion in circulating and frontal systems, convection, wrapping etc. Wind causes water and energy transport, increases evaporation intensity, withdraws heat, acts with dynamic pressure and has influence on snowdrift and frost creation. Wind velocity, wind speed fluctuates. Wind direction is given in azimuth degrees from 0 - 360. Wind speed and direction is derived also from effect of wind pressure on objects. (Beaufort scale with 13 degrees characterises effects of ground wind – cca 7-10 m above the ground). In low altitudes the wind speed reaches its maximum around 14h and minimum during the night or morning. In altitudes 500 m a.s.l. and higher these peaks are reverse. Wind speed is measured in m s^{-1}.

4.2.15 Photosynthetically active radiation

The Photosynthetically Active Radiation (PhAR) measure of radiant power is important in evaluating the effect of light on plant growth. It was shown by McCree (1972) that the photosynthetic response correlates better with the number of photons than with energy. This is expected because photosynthesis is a photochemical conversion where each molecule is activated by the absorption of one photon in the primary photochemical process. PhAR is defined in terms of photon (quantum) flux, specifically, the number of moles of photons in the radiant energy between 400 nm and 700 nm. One mole of photons is $6.022\ 141\ 29 \cdot 10^{23}$ (Avogadro's constant). The Photosynthetic Photon Flux Density

(PPFD), i.e., the photon irradiance, is expressed in moles per square meter and per second (value twice more than Watts), formerly, Einsteins per square meter and per second. The data obtained from datalogger were in μmol per square meter per second (a common unit for a photon flux), thereby we had to convert the values for our scale three orders higher into mol per square meter per second. Installation of PhAR sensor DC50 B2 above the vegetation was on June 25th 2013.

4.3 Data processing

The data were processed using Mini 32 software version (402.53) made by EMS Brno. This software is fully compatible with all the measuring devices used. The data were processed and evaluated with Mini32 software, which enables data editing, computation, extrapolation and numerous statistical evaluations. The temperature sensors were calibrated through the wide scale of temperatures (5 – 25°C) in the growth chamber. Final data were exported into MS Excel for the graphical purposes and clarity.

5 Results

Comparison of actual evapotranspiration values measured both by BREB method and the sap flow. Simultaneous use of these methods provides also the verification of the results obtained. Traditionally, the averaging time for the BREB technique is 30min – 1h (Steduto & Hsiao (1998). For our purposes we used the two term intervals. To the longer term period are linked the mean and total values in 24 h-intervals. Short terms, 10min interval values, were used to display more detailed dynamic physiological responses of the plant to canopy fluxes. Data sets are in the Table 8.3.3a.

5.1 Diurnal analysis

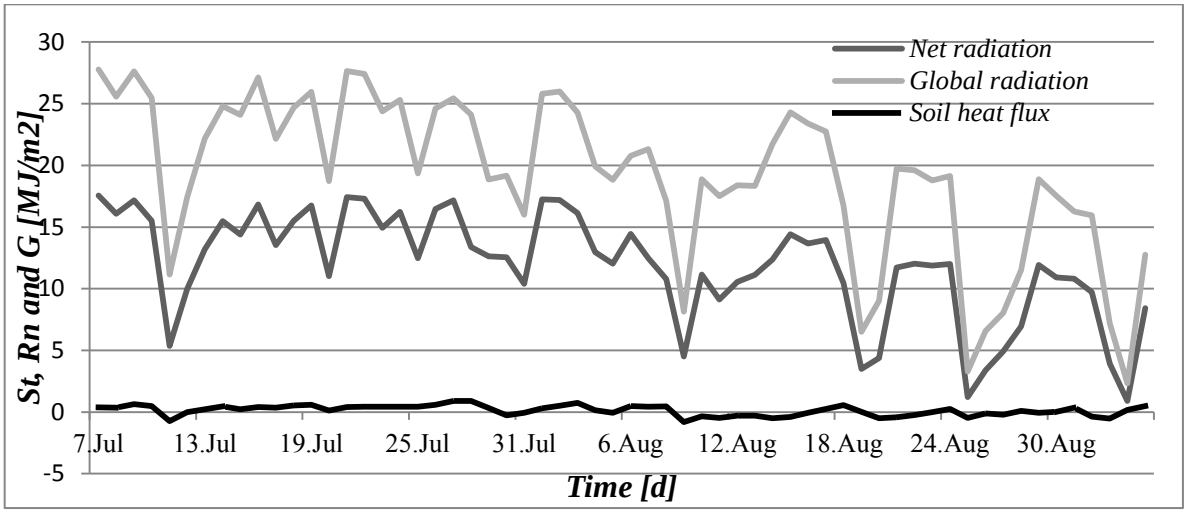

Fig. 5.1.: Global radiation, net radiation and soil heat flux.

The comparison of global radiation, net radiation and the soil heat flux can be celarly seen in Fig. 5.1. As the canopy developes, the heat flux into the soil is lower and lower. Especially when the sky is obscured. Daily total of radiation balance - net radiation (R_n) - represents approximattely 50% of Solar total radiation - global radiation (R_g). Values in 10 minutes interval illustrates negative sign of R_n during the night time period due to energetic loss by greater otput than input - emmision – of energy, longvawe radiation.

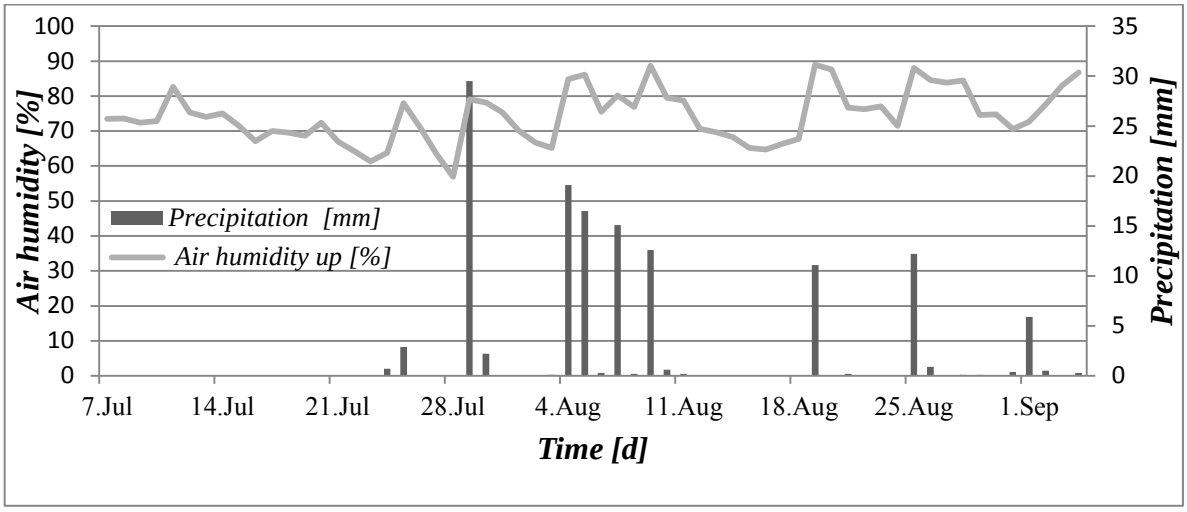

Fig. 5.2.: Air humidity and precipitation.

June 2013 was represented the typical sunny weather with seldom occurrence of summer storms. In the end of the month a pressure low brought a wave of extensive rainfalls and minor flood situations. In the beginning of August 2013 the weather had a tropical character and in the rest of the month summer weather with irregular precipitation and convective character prevailed.

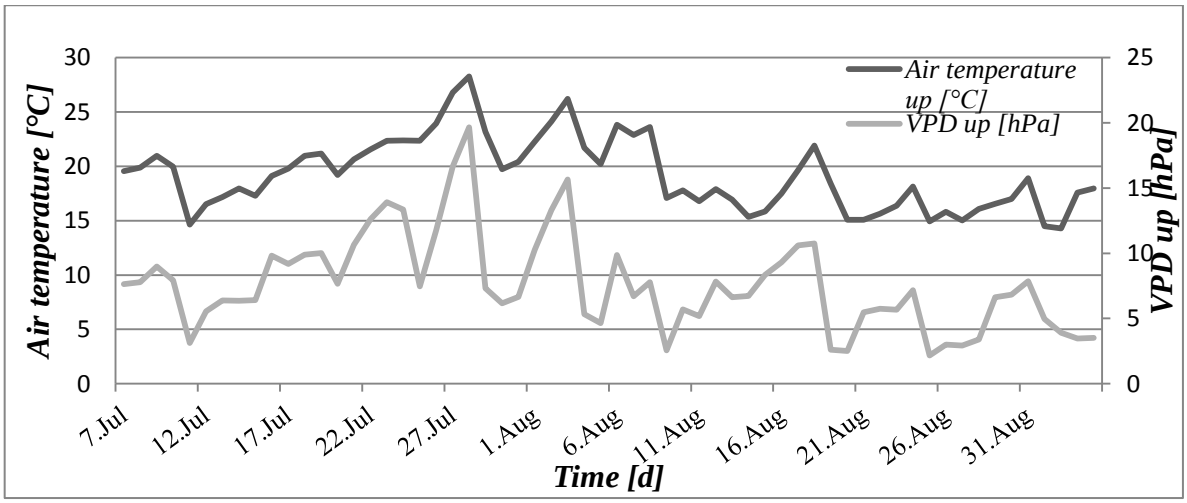

Fig. 5.3.: Air temperature and VPD.

Fig. 5.3: Shows the close dependency of the air temperature on vapour pressure deficit. In the end of June the average temperature approached tropical character. Character of weather in August 2013 was average.

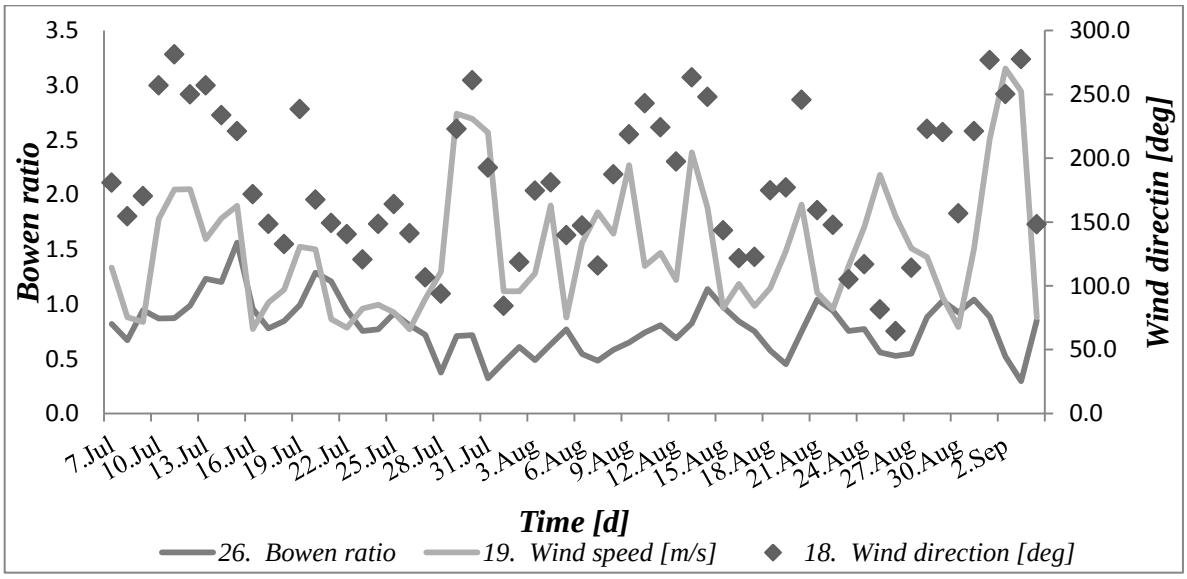

Fig. 5.4.: Bowen ratio, wind speed and wind direction.

Wind is important factor for PET calculation. Wind influences on PET by 20% in the actual measurement.

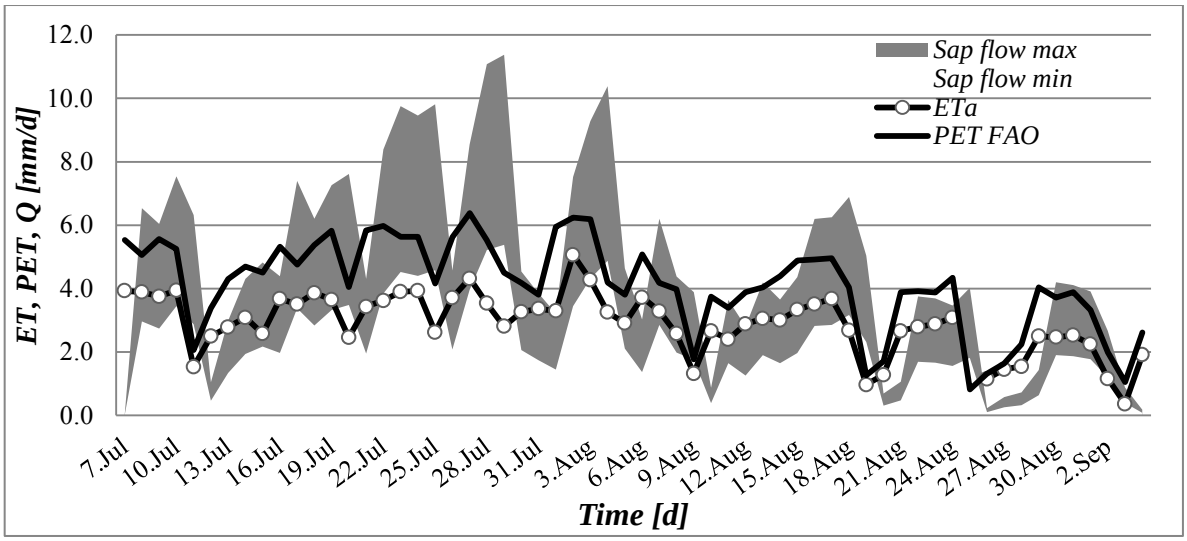

Fig. 5.5.a: Potential and actual evapotranspiration and sap flow. The source data are displayed Table 8.3.4a and Table 8.3.4.b.

From the graph it is obvious, that even the minimal measured values (white coloured area in the graph) of the sap flow exceed the evapotranspiration rate, not mentioned the maximal measured values of sap flow (dark grey coloured area).

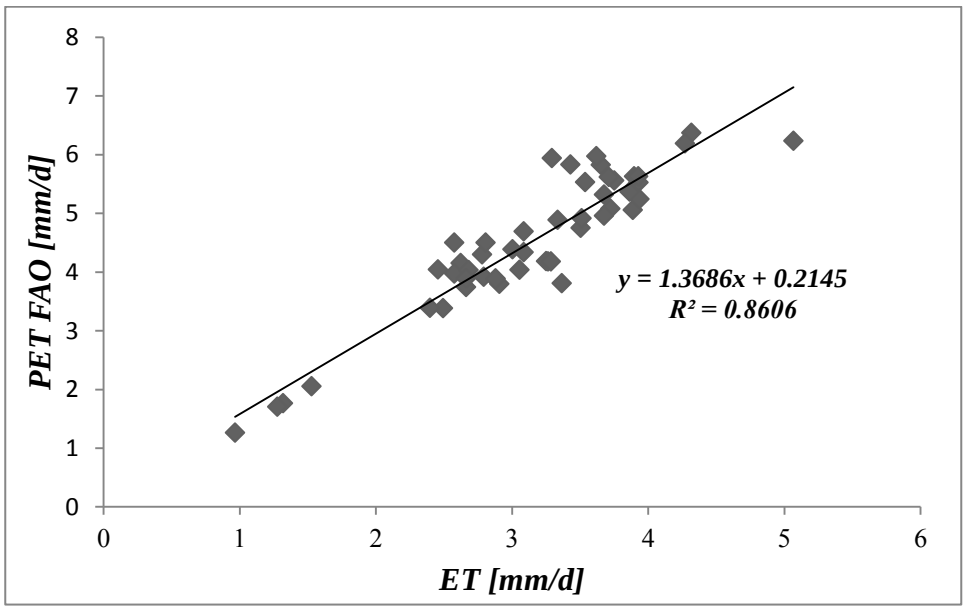

Fig. 5.5b: Linear regression of potential and actual evapotranspiration.

The graph (Fig. 5.5b) shows close correlation of the values of actual evapotranspiration and potential evapotranspiration calculated according to FAO. Potential evapotranspiration appears as by more than 30 % greater than the actual one.

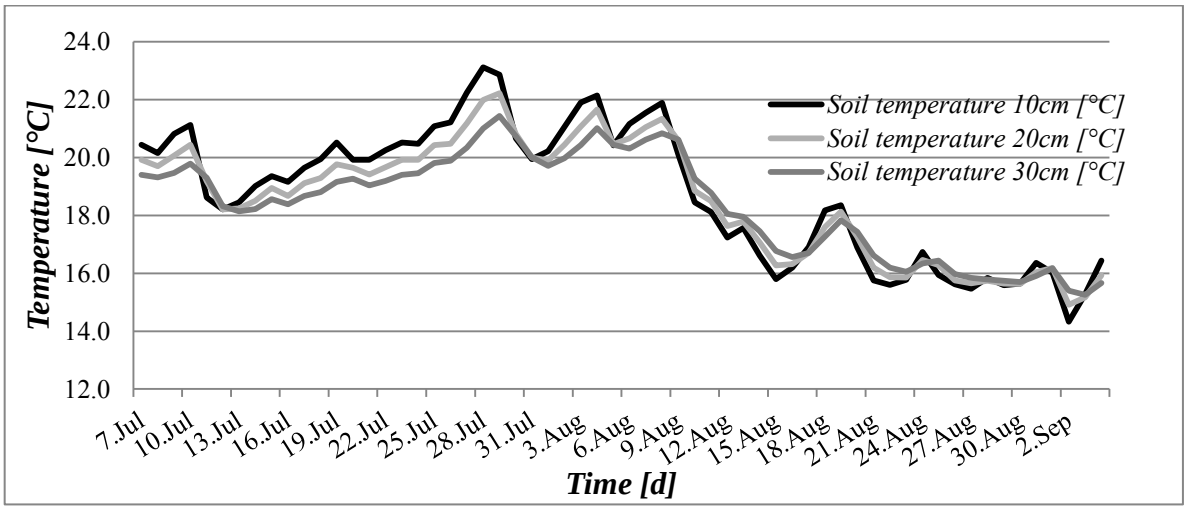

Fig. 5.6.: Soil temperature at three different depths.

Soil temperature has two main features – time shift and decreasing amplitude with the increasing depth. Soil temperature influences important processes as weathering and soil formation; water and air regime; germination and growth of plants and activity of soil organisms. Temperature optimum for most of organisms is 10-35℃.

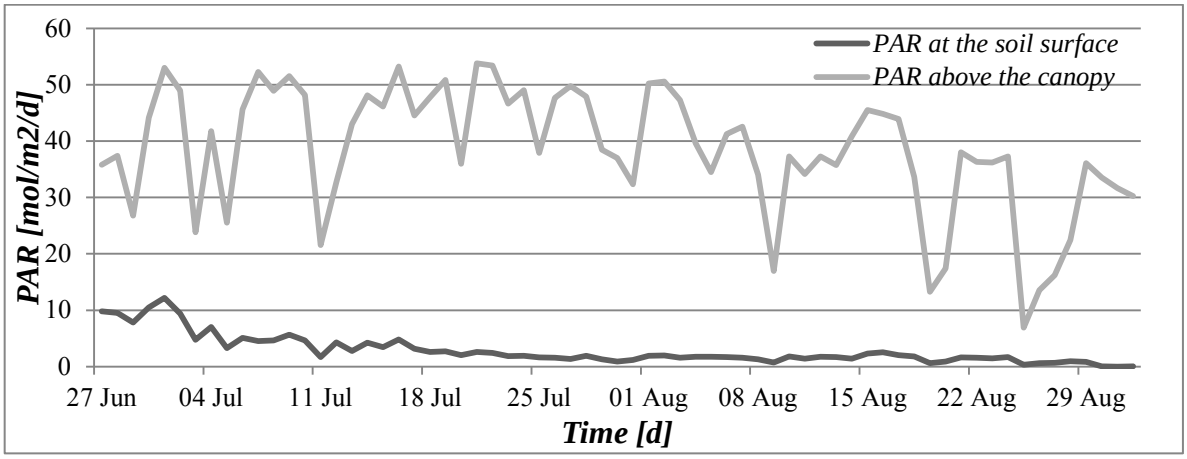

Fig. 5.7.: Amount of photosynthetically active radiation above and inside the crop canopy.

The corn (*Zea Mays L.*) was the dominant species in the site and created most of its canopy (Photo 8.3). Possible presence of the weed species within the canopy was negligible and was not taken into an account as an important variable for the purposes of the data evaluation. Leaf area development modifies the penetration of the radiation into the canopy and which impacts the growth under the active canopy layer. The calculated methods according to PET FAO and BREB technique, the correlations are displayed in the appendices Fig.5.7.1.

5.2 10-minutes analysis

The loss of the fine features of the flux data using 24h-interval is significant. It is necessary to take in account that the mean daily values may be sufficient for the period observation, but the output from the dataset consisting from 10min-interval values enable to display the diurnal energy fluctuations and dependencies. Maximal and minimal values correlating with the evapotranspiration are represented in the Fig. 5.8. Based on the theory, that the transpiration would be the highest during the warm, sunny day, the date July 2013 (sunrise 05:03, sunset 21:11, length of the day 16h 07m 58s − 1m 34s, Solar noon 13:08 altitude 62,2°). The graph displays transpiration minimum and maximum values (after recalculation to $mm \cdot m^{-2} \cdot day^{-1}$). Air humidity together with *Rn* are used for the sap flow calculation. Air humidity affects the vapor pressure gradient of the atmosphere and wind mixes and alters the vapor pressure gradient. A transpiration peak at the beginning of radiation resulting in evaporation of this condensed water. Additional problems result from leaf wetting by precipitation. In this case, the precipitation could be neglected as supported by the Fig 5.9. According to this fact, the the increment of the morning transpiration is the evaporation of the morning dew condensed on the leaf. Sap flow linear regression of measured and calculated is presented in the Fig. 5.10. In the upper graph, there is the fitting of the maximal values and in the lower, the fitting of the minimum values. Correlation is very close between the values from the calculated and measured method. The scale on y-axis shows that the maximal values were nearly as twice as bigger than the minimal. The possible reasons of the difference are described in the discussion.

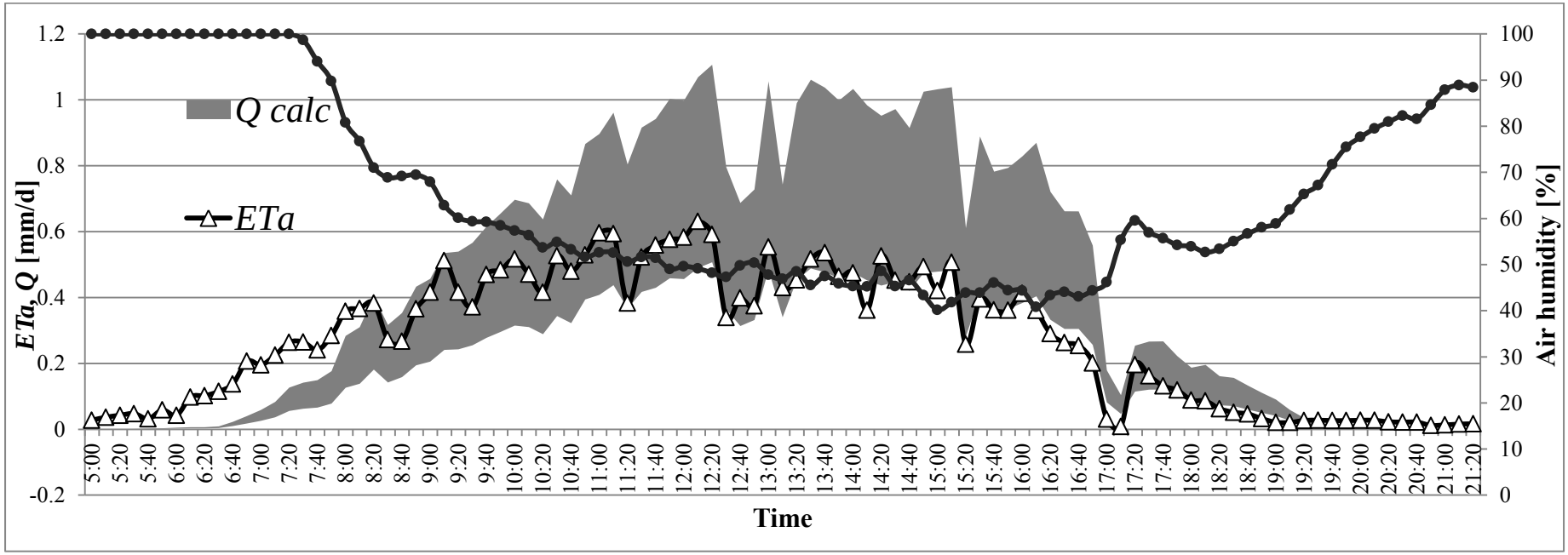

Fig. 5.8.: The relationship of calculated sap flow (*Q calc*), actual evapotranspiration (*Eta*) and relative air humidity in 10-min interval from the sunrise till the sunset.

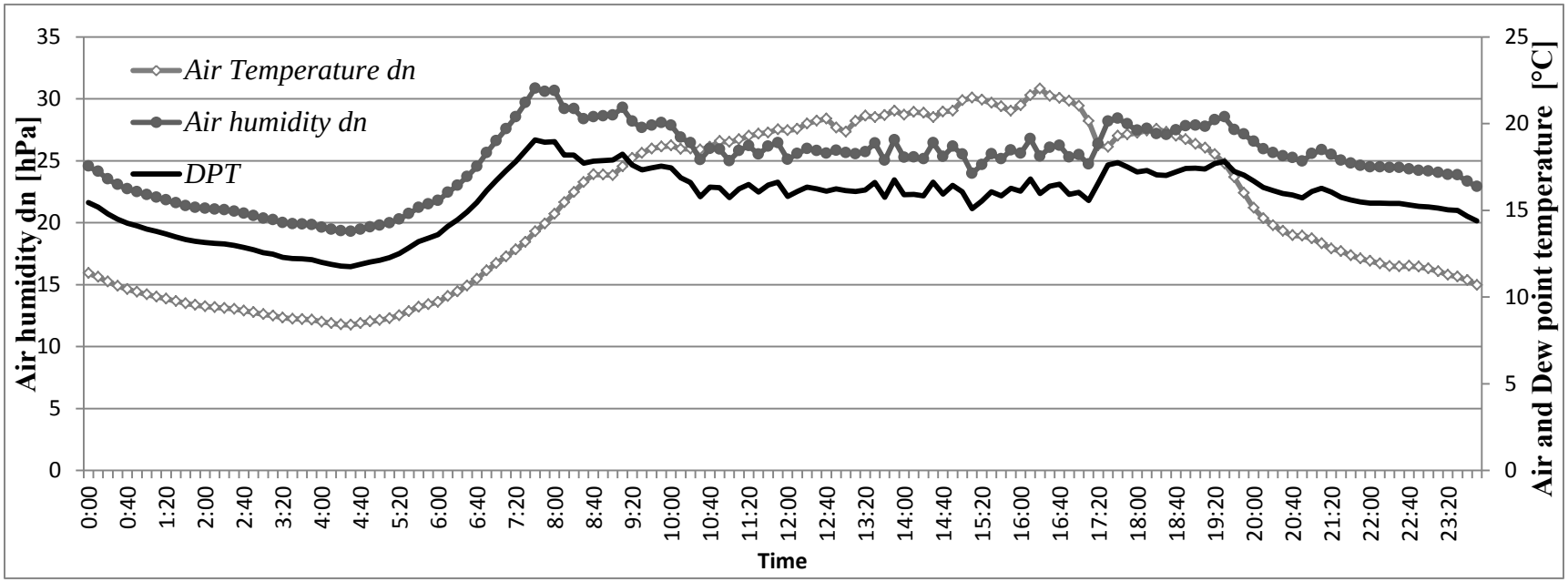

Fig. 5.9: Air temperature, air humidity and dew point temperature.

Fig. 5.9. is relating to the previous graph (Fig 5.9) in the same time scale and describes the dependency of the air temperature on air humidity and dew point temperature. Root water uptake and sap flow continued after stomata have closed in the evening and transpiration has stopped. For this reason, the water deficit in the plant, having risen during the day, was nearly replenished until midnight.

6 Discussion

The results from the presented methods show clearly, that they are both suitable for estimating that the evapotranspiration of the corn canopy. The results are clear and convincing. Interesting finding was the fact that the transpiration overcomes the evaporation (Fig. 5.9). Simple explanation to this fact can be that the plants chosen for the measurement were transpirating in a higher rate. Campbel and Reece (2006) claim, that the degree of transpiration will be probably the highest in sunny, warm, dry and windy day, as these factors increase the water evaporation. The meteorological conditions for the time period of the measurements can be obtained from the Fig. 5.2. The weather conditions are corresponding to the claim above and thereby this can be stated as another answer why the transpiration was higher than evapotranspiration. After the rain the rate of evapotranspiration could be increased by the evaporating of the water from the leaf which was intercepted on its surface. From the Fig 5.8 is obvious the high rate of the transpiration in the morning hours. This was described by Čermák et al. (1994), who suggested, that for transpiration in morning hours, plant uses the water from the tissue storage. The density of crop canopy also plays important role. As the plant grows, the canopy gets denser and due to the leaf development and increment of the leaf area, shading of the adjacent plants can contribute to the decrease of received energy. This may result in lower evapotranspiration rate. There is also a difference between the minimal and maximal sap flow. Regarding the credibility of the measurements, when the energetic requirements are not exceeded, the values are real. In other words, the rate of evapotranspiration is not bigger than the energy from incoming radiation. Evaporating water could be recalculated into latent heat. Latent heat consumed for evaporation. Sensible heat is the convective heat consumed for heating. These two fluxes are parts of the net radiation (equation 16). Another factor affecting the measurements is the properties of the applied devices. Measurements of sap flow with surface mounted thermocouples are very sensitive to ambient thermal influences (von Willert et al., 1995). The thermal contact between the stem and sensor is particularly important and frequently interrupted by penetration of water between the heaterstrip and the stem and by the growing stem. Therefore the sensors have to be moved often to another plant. (Kjelgaard et al., (1997) and Jara et al. (1998) confirm, that sap flow measurements at the same plant are practicable until one week in dependence of weather conditions and stem

thickening. Under the weather conditions on the site of the sap flow were favourable and the measurements of sap flow were made on the same plants throughout whole experimental period. Another issue is the upscalling, as claims Merta et al. (2001), limitations lie in the difficulties, and the impossibility of measurements of the absolute actual transpiration rates of agricultural crops for longer periods like months or years. The upscalling (from a single leaf) to the whole plant and finally to the canopy would lead to larger error. As confirm Köstner et al. (1996), the gas exchange and sap flow methods, upscalling from leaf to plant canopy is difficult to do because measurements with this methods reflect only reactions of single plants. They always represent only a facet of micro scale adds Merta et al (2001). Paraphrasing Čermák et al. (2004) the up-scaling from a series of individual plants to stands should be done with respect to existing natural variation between plants under given environmental conditions. It is suitable to apply, both at the individual plant as at the whole canopy levels, the available biometric parameters; which is also in concordance with the claims of Čermák et al. (2004). To mitigate the issues associated with up-scaling, I suggest, the sufficiently high number of sample plants and proper integration techniques. When extrapolating from the small amount of data, the approximation of the obtained data is relative and dependent on many factors. The more relevant data and variables are available, the more precise the data output will be. In our case, the limiting factor was number of sensors. If the experimental samples are not numerous, there is important to maintain the favourable conditions for the measurement and the applied devices. We came to an agreement with the conclusion of Steduto & Hsiao (1998). The noise of or autocorrelation due to the use of one flux to calculate another was ruled out by very high coincidence in the fluctuations among related parameters measured independently by different instruments. Steduto & Hsiao (1998) also sums up that the direction and extent of fluctuations under changing solar radiation are consistent with theories of energy balance and transport. Together with keeping high surveillance on the measuring devices to prevent an interruption of the field measurements, this would lead to more efficient obtaining of data for further evaluation. Even though the testing the accuracy of the methods under a new set of conditions is laborious, time-consuming and costly, and yet evapotranspiration data are frequently needed at short notice for project planning or irrigation scheduling design (Allen et al. 1998), the closer evapotranspiration modeling might improve crop water consumption control. In comparison to the sap flow method, the output of the BREB showed much lower energy flux. According to Stannard (1996), BREB

can be reduced by lowering the lower sensor, as well as by the lowering the upper sensor. However I lean to the view, that the energy flow was low because the incoming energy was low. Steduto & Hsiao (1998) say the BREB technique is based on gradient transport and does not reflect the turbulent nature of the underlying processes, so it has been viewed with skepticism. In experimental measurements an adequate fetch is required, in order to have confidence that the heat fluxes were in equilibrium with the surface. Nevertheless, sometimes the measurements can give incorrect signs for those fluxes, at least for the estimates provided by BREB method (Perez et al, 1999). On the other hand Prueger et al. (1997) concludes, the Bowen-ratio technique provide good estimates of evapotranspiration over larger areas than is possible with lysimeters. Steduto & Hsiao (1998) sums up, that Bowen technique is apparently as effective as the other measuring techniques, when the upper and the lower parts placed sufficiently apart within the adjusted boundary layer above relatively smooth canopies - as is our corn crop field – and with proper time averaging. The BREB technique method is capable to resolve the rapid changes in fluxes which are brought about the canopy responses to the radiation and other environmental factors. Issues connected with the features of vascular bundles and plant physiology can be also responsible for the scenario when the transpiration exceeds evapotranspiration. The certain amount of water can be retained within the vascular bundles, which consequently leads to the fact, that amount of water output can be lower than the amount of water gained by the plant through the root system from the soil. Hydraulic capacitance buffers a change in flow and tension in the xylem by increasing the time required the time required for a response to a perturbation to be completed (Phillips et al., 2004). Some large trees could have relatively small hydraulic time constants while small plants could have relatively large time constants (Hunt et al., 1991, Phillips et al. 1997). Diverse plant forms can have any combination of a large hydraulic resistance and large hydraulic capacitance (e.g. Tall tropical trees); small resistance and small capacitance (e.g. young phreatophytes), large resistance and small capacitance (e.g. desert shrubs) and small resistance and large capacitance (e.g. desert succulents). Because a plant's characteristic hydraulic response time is a product of effective hydraulic resistance and capacitance, plants may show a variety of hydraulic response times based on different underlying mechanisms and adaptations (Phillips et al. 2008). Another physiological problem is the water diffusion into ambient atmospheric layer – resp. dependence on the surface resistance of the plant or canopy. For the better accuracy of the data, knowledge about turbulent diffusion and

another aerodynamical characteristics of the crop surface should be also taken into an account. To support the interpretation of sap flow and gas exchange measurements I suggest, according to Merta et al. (2001), to measure also the leaf water potential which allows to assess the plant water status and the response of plants to evapotranspiration demand and soil moisture content. The measurements are eminent for better understanding of the role of plants in the soil water balance and as a basis of model development (Peschke et al. 1997, Yu et al., 1998). Köstner et al. 1996 and Peschke et al 1997 agree, that the simultaneous use of several physiological methods facilitates interpretation of water transport through plants. Merta et al. 2001 sums up that these methods are not suitable to quantify actual evapotranspiration rates for longer periods like months or years. In the arid areas (e.g. Northern China), where the water for an extensive irrigation is obtained mainly by pumping from deep wells, the water table declines rapidly which can lead to soil salinization. Depletion of the underground water resource is forcing agriculture to find more efficient use of water. This was investigated and proved by Zhang et al. (1998), that the single irrigation could avoid sever leaf water deficit at the later stages of growth. One-time irrigation was combined with the late sowing and high sowing density, which lead to development of the deeper root system of the plants. In the surface layer, 0-20 cm, soil water potential fluctuated as a function of the rainfall and irrigation. Reduced irrigation promoted root expansion deep in the soil profile. Zhang et al. (1998) propose, that the roots in the dry upper soil work as a soil-drying sensor and regulate stomatal conductance and leaf elongation rate. Jones (1980) and Cowan (1982) pointed out, such a regulation is essential for plant survival under unreliable rainfall and may be described as a feed-forward mechanism, in contrast to the feed-back mechanism with which a leaf water deficit induces stomatal closure and growth inhibition. Less irrigation resulted in significantly less leaf area development Zhang et al. (1998) and reduced the yield. Single-irrigation system can contribute to sustainable agriculture in arid regions in terms of water consumption. Such irrigation could prevent the further reduction of the underground water resource and at the same time make better use of rain. Magnitude of the water deficit and the type of soil conditions the soil water content. Allen et al. (1998) claims, the too much water will result in waterlogging which might damage the root and limit root water uptake by inhibiting respiration. At a certain critical time, uptake will switch from plant-atmosphere demand driven to soil supply dependent. Crop water consumption can be described from the local scale, to the field scale and to the regional and global scales. The local model can be

incorporated in SPAC (Soil-Plant-Atmosphere Continuum) numerical models which can be used for uspscalling, like: SWAP, HYSWASOR, HYDRUS, ENVIRO-GRO and FUSSIM.

7 Conclusions

The comparison of the BREB and sap slow methods showed, that both methods are suitable for the estimation of the evaporation. Diverse plant forms can have any combination of a large hydraulic resistance and large hydraulic capacitance. When estimating the sap flow for the whole canopy, it has to be taken into an account, that upscalling from leaf to plant canopy is difficult to do because measurements with this methods reflect only reactions of single plants. To mitigate the issues associated with up-scaling, I suggest, the sufficiently high number of sample plants and proper integration techniques. For the maize plant the results shown presence of small time shifts in both phenomena, thereby it is possible to roughly estimate the canopy water supply from the comparison of BREB and sap flow.When the transpiration exceeds the transpiration, it is either due to the evaporation of the due condensed on the leaf surface or after the precipitation, from the evaporation of the intercepted water on the leaf. The methods are useful in assessing the water balance of the site.

8 Appendices

8.1 Abbreviations and symbols

ET	Evapotranspiration
PET	Potential evapotranspiration
BREB	Bowen ratio energy balance
calc	Calculated
IPAR	Incident photosynthetically active radiation
$IPAR_i$	Intercepted photosynthetically active radiation
PhAR	Photosynthetically active radiation
RUE	Radiation use efficiency
RuBP	Ribulose-1,5-bisphosphate carboxylase/oxygenase
VPD	Vapour pressure deficit
HI	Harvest index
sw	Shortwave
lw	Longwave

Table 8.1.: Used abbreviations and symbols.

8.2 Parameters and Units

Parameter	Description	Unit
$ß$	Bowen ratio	[-]
κ	thermal diffusivity	$m \cdot s^{-1}$
ρ_s	density of the soil	$g \cdot m^{-3}$
ρ_v	density of water	$g \cdot m^{-3}$
Φ	osmotic coefficient	[-]
Ψ	water potential	$J \cdot kg^{-1}$
Ψ_m	matric potential	kPa
λ	latent heat of vaporization of water	$J \cdot g^{-1}$
λE	latent heat flux	$W \cdot m^{-2}$
χ	absolute humidity or vapour density	$g \cdot m^{-3}$
γ	thermodynamic psychrometer constant	$hPa \cdot °C^{-1}$
Θ	volumetric water content	$cm^3 \cdot cm^{-3}$
c_s	soil specific heat	$J \cdot kg^{-1} \cdot °C^{-1}$
c_p	specific heat of moist air at constant pressure	1004 $J \cdot kg^{-1} \cdot °C^{-1}$
ΔT	difference in temperature	°C
Δz	difference in height	m
e_a	actual vapour pressure of air	kPa
e_i	efficiency of interception	[-]
e_s	saturation vapour pressure of water depending on temperature	kPa
G	gravitational constant	9.81 $m \cdot s^{-2}$
g_{Ha}	heat conductance	$mol \cdot m^{-2} \cdot s^{-1}$
g_v	vapour conductance or boundary conductance for the whole leaf	$mol \cdot m^{-2} \cdot s^{-1}$
G	soil heat flux	$W \cdot m^{-2}$
Rh	relative humidity	%
H	is the sensible heat loss	$W \cdot m^{-2}$

k	von Karman's constant	0.41 [-]
k	thermal conductivity	$W \cdot m^{-1} \cdot K^{-1}$
K_v	eddy transfer coefficient for water vapour	$m\text{-}^{2} \cdot s\text{-}1$
K_h	eddy transfer coefficient for heat	$m^{2} \cdot s\text{-}1$
K	hydraulic conductivity	dimensionless
L_d	downward radiation	$W \cdot m\text{-}^{2}$
L_{oe}	emitted thermal radiation	$W \cdot m\text{-}^{2}$
L_u	upward radiation total irradiance on the lower surface	$W \cdot m\text{-}^{2}$
N	shoots biomass	Kg
N_A	Avogadro's constant	$6.02214129(27) \times 10^{23}\ mol^{-1}$
P	the pressure	Pa
p *	the heat input power	W
p_a	the atmospheric pressure	kPa
Q	sap flow rate	$kg \cdot s^{-1}$
R	the gas constant	$8.314\ J \cdot mol^{-1} \cdot K^{-1}$
R_{abs}	absorbed radiation	$W \cdot m^{-2}$
r_l	bulk stomatal resistance of the leaf	$s \cdot m^{-1}$
r_s	bulk (surface) resistance	$s \cdot m^{-1}$
R_n	net radiation flux	$W \cdot m^{-2}$
S_b	scattering irradiance on the leaves	$W \cdot m^{-2}$
S_d	scattering irradiance on the ground	$W \cdot m^{-2}$
S_p	irradiance from the sun	$W \cdot m^{-2}$
S_{tr}	is the total reflected radiation	$W \cdot m^{-2}$
T	Kelvin temperature	K
T_a	is the air temperature	°C
T_L	is the leaf temperature	°C
u	wind speed	$m \cdot s^{-1}$
u	rate of water uptake from the soil	$mm \cdot h^{-1}$
v	flow velocity	$m \cdot s^{-1}$

Table 8.2.: Used parameters, their description and their SI-based and derived units.

8.3 Figure and table captions

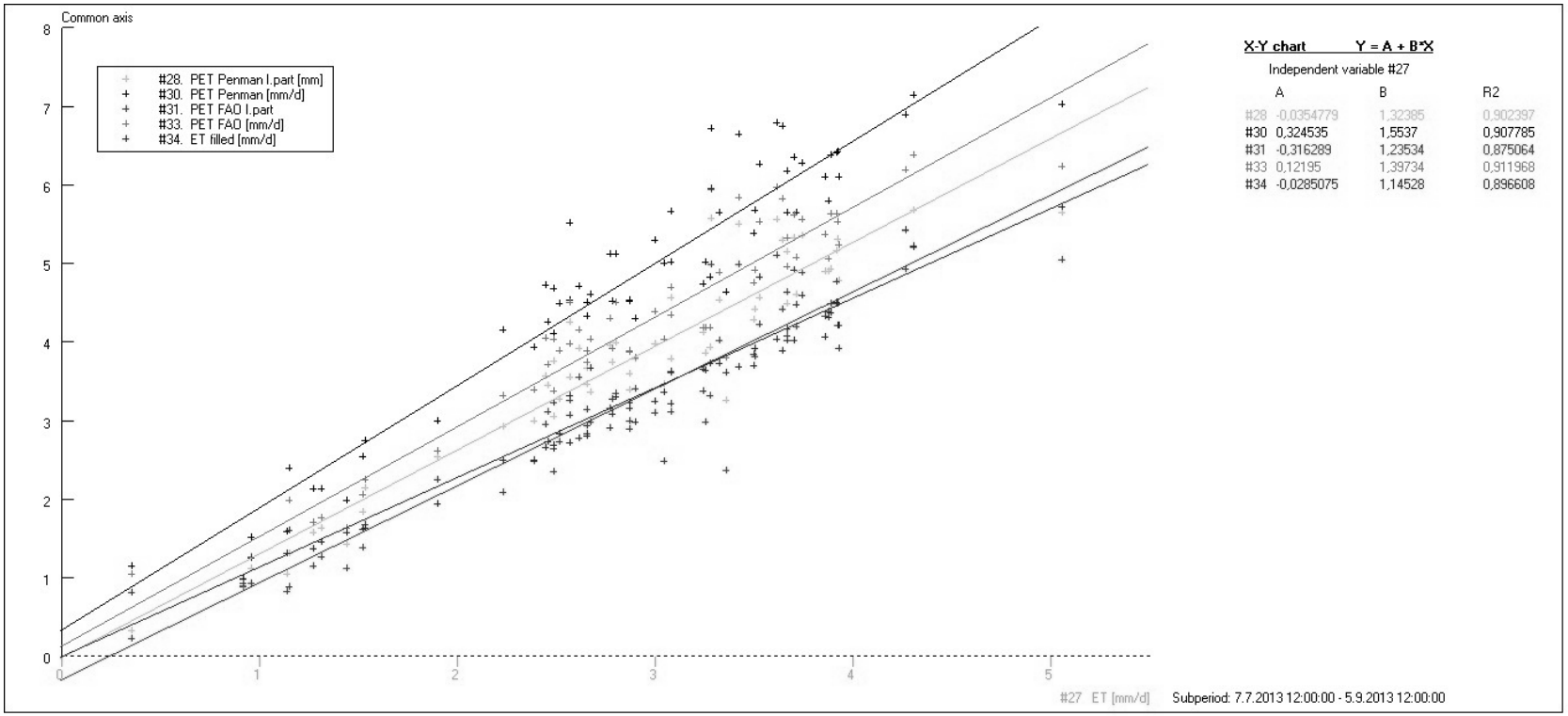

Fig. 5.7.1: Correlation of PET Penman, PET FAO and BREB.

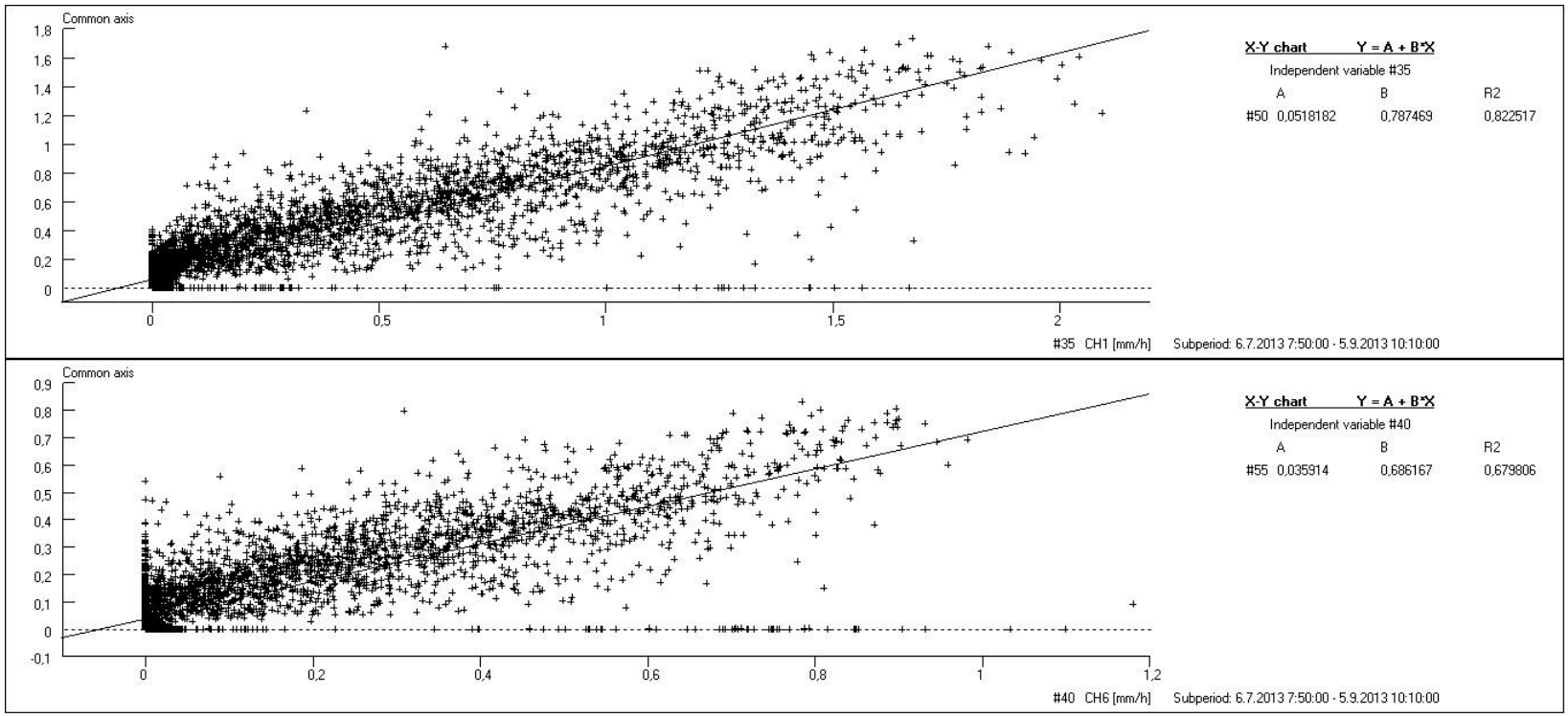

Fig. 5.10 Measured and calculated **s**ap flow linear regression.

Time period: 6.7.2013 7:50:00 - 5.9.2013 10:10:00

Var.	Description	Min	Max	Average	Records	Total	Std. dev.
#1	Precipitation SR03 [mm]	0	4,2	0,01499034	8799	131,9	0,1091208
#2	Soil temperature 10cm [°C]	13,54336	25,10425	18,75313	8798	164990	2,657756
#3	Soil temperature 20cm [°C]	14,57203	25,10628	18,53949	8798	163110,4	2,111873
#4	Soil temperature 30cm [°C]	15,15304	27,68266	18,36729	8798	161595,4	1,790652
#5	SWP 10cm [kPa]	8,714305	169,3	97,98841	8798	862102	58,1373
#6	SWP 20cm [kPa]	8,002611	169,3	109,4946	8798	963333,3	53,72778
#7	SWP 30cm [kPa]	7,767132	169,3	131,08	8798	1153242	49,95732
#8	VWC 10cm [m3/m3]	-0,1836367	0,3896737	0,3406844	8798	2997,341	0,02225296
#10	VWC 30cm [m3/m3]	-0,2841478	0,3306901	0,2990358	8798	2630,917	0,02116518
#11	Air temperature up [°C]	5,9195	38,506	19,22068	8798	169103,5	5,846123
#12	Air humidity up [%]	27,367	100	74,5001	8798	655451,8	20,96974
#13	Air temperature dn [°C]	5,33	39,406	19,30154	8798	169814,9	6,403949
#14	Air humidity dn[%]	27,8765	100	76,14572	8798	669930	21,68785
#15	Net rad. balance [W/m2] #8407	-94,15987	749,3798	138,293	8798	1216701	209,2057
#16	Global rad. [W/m2] #2624	0	1069,727	223,661	8798	1967769	281,8608
#17	Soil heat flux 10cm [W/m2] #13	-162,2216	43,90427	1,512931	8798	13310,76	15,31789
#18	Wind direction [deg]	0,250624	353,6988	177,4285	8798	1561016	92,02397
#19	Wind speed [m/s]	0,28	9,81354	1,504619	8799	13239,14	1,054132
#20	VPD up [hPa]	0	45,75338	7,579872	8798	66687,72	8,020708
#21	Air humidity up [hPa]	8,691143	26,05447	16,02224	8798	140963,7	3,180408
#22	VPD dn [hPa]	0	45,25054	7,554436	8798	66463,93	8,55042
#23	Air humidity dn [hPa]	8,918502	33,34988	16,44125	8798	144650,1	3,43003
#24	dT [deg.C]	-4,319499	3,890499	0,0808565	8798	711,3755	0,8922948
#25	de [hPa]	-2,496995	7,295411	0,4190115	8798	3686,463	0,7476689
#26	Bowen ratio	0,100035	3,964648	0,8182688	5888	4817,967	0,5299071
#27	ET [mm/h]	0	0,8405193	0,2434063	4331	1054,193	0,1707494
#28	PET Penman I.part [mm]	0	0,8134253	0,157452	8798	1385,263	0,2095984
#29	PET Penman II.part [mm]	0	0,1912667	0,04263916	8798	375,1393	0,04029306
#30	PET Penman [mm/h]	0	0,9723918	0,2000912	8798	1760,402	0,2390498
#31	PET FAO I.part	0	0,7185409	0,134889	8798	1186,753	0,1813805
#32	PET FAO II.part	0	0,2123279	0,03784173	8798	332,9315	0,03999366
#33	PET FAO [mm/h]	0	0,8182512	0,1727307	8798	1519,685	0,2073624
#34	ET filled [mm/h]	0	0,8405193	0,1361521	8798	1197,866	0,1665872

Table 8.3.3a) 10 minutes interval statistics of the whole set of variables - 1st part.

Time period: 6.7.2013 7:50:00 - 5.9.2013 10:10:00

Var.	Description	Min	Max	Average	Records	Total	Std. dev.
#35	CH1 [mm/h]	0	2,097001	0,2365424	6134	1450,951	0,4014735
#36	CH2 [mm/h]	0	1,631223	0,1670575	6190	1034,086	0,2814452
#37	CH3 [mm/h]	0	1,677443	0,156415	6120	957,2595	0,264557
#38	CH4 [mm/h]	0	1,384824	0,1431708	6020	861,888	0,2453032
#39	CH5 [mm/h]	0	1,684246	0,1706336	6270	1069,873	0,2840082
#40	CH6 [mm/h]	0	1,180789	0,108936	6042	658,1911	0,195166
#41	CH7 [mm/h]	0	1,571162	0,1908658	5943	1134,316	0,2903499
#42	CH8 [mm/h]	0	1,952479	0,1171319	6112	715,91	0,2456731
#43	CH9 [mm/h]	0	1,39117	0,1664623	6003	999,2729	0,2531212
#44	CH10 [mm/h]	0	1,870356	0,2211845	6282	1389,481	0,3637678
#45	CH11 [mm/h]	0	1,689546	0,2052885	6118	1255,955	0,3169434
#46	CH12 [mm/h]	0	1,285329	0,1585114	6136	972,6258	0,2397111
#47	Global rad. [W/m2] #2624	0	1069,727	223,661	8798	1967769	281,8608
#48	VPD up [hPa]	0	45,75338	7,579872	8798	66687,72	8,020708
#49	VPD dn [hPa]	0	45,25054	7,554436	8798	66463,93	8,55042
#50	CH1 calc [mm/h]	0	1,730268	0,2018351	8798	1775,745	0,3214357
#51	CH2 calc [mm/h]	0	1,326811	0,1529168	8798	1345,362	0,2438526
#52	CH3 calc [mm/h]	0	1,618837	0,1895171	8798	1667,371	0,3016815
#53	CH4 calc [mm/h]	0	1,026051	0,1128822	8798	993,1374	0,1818041
#54	CH5 calc [mm/h]	0	1,303742	0,1461634	8798	1285,946	0,2334517
#55	CH6 calc [mm/h]	0	0,8310782	0,0922534	8798	811,6454	0,1486924
#56	CH7 calc [mm/h]	0	1,310861	0,1528008	8798	1344,341	0,2432649
#57	CH8 calc [mm/h]	0	1,116068	0,1288953	8798	1134,021	0,2058296
#58	CH9 calc [mm/h]	0	1,247607	0,1467525	8798	1291,128	0,2330759
#59	CH10 calc [mm/h]	0	1,683028	0,1984119	8798	1745,628	0,314893
#60	CH11 calc [mm/h]	0	1,577188	0,194626	8798	1712,32	0,3059262
#61	CH12 calc [mm/h]	0	1,020479	0,1245048	8798	1095,393	0,1956325
#62	DPT dn [°C]	5,33	25,88745	14,16403	8798	124615,1	3,208913

Table 8.3.3b) 10 minutes interval statistics of the whole set of variables - 2nd part.

Time period: 7.7.2013 12:00:00 - 4.9.2013 12:00:00

Var.	Description	Min	Max	Average	Records	Total	Std. dev.
#1	Precipitation SR03 [mm]	0	29,5	2,195	60	131,7	5,667905
#2	Soil temperature 10cm [°C]	14,32637	23,1124	18,74412	60	1124,647	2,322148
#3	Soil temperature 20cm [°C]	14,90713	22,21483	18,5362	60	1112,172	2,030113
#4	Soil temperature 30cm [°C]	15,25451	21,43551	18,36773	60	1102,064	1,767902
#5	SWP 10cm [kPa]	9,373206	169,3	98,26663	60	5895,998	57,97887
#6	SWP 20cm [kPa]	8,374976	169,3	109,5589	60	6573,534	53,00872
#7	SWP 30cm [kPa]	8,995516	169,3	131,0334	60	7862,004	49,46845
#8	VWC 10cm [m3/m3]	0,3189041	0,381387	0,3409296	60	20,45577	0,01606864
#10	VWC 30cm [m3/m3]	0,2802547	0,3283675	0,2993675	60	17,96205	0,01397872
#11	Air temperature up [°C]	14,27311	28,25339	19,23767	60	1154,26	3,271453
#12	Air humidity up [%]	56,89346	88,95135	74,34279	60	4460,567	7,476034
#13	Air temperature dn [°C]	14,25451	28,22472	19,30591	60	1158,355	3,296082
#14	Air humidity dn[%]	61,07542	90,64027	76,03033	60	4561,82	6,638588
#15	Net rad. balance [MJ/m2] #8407	0,8982353	17,55571	11,87474	60	712,4843	4,317879
#16	Global rad. [MJ/m2] #2624	2,338962	27,77696	19,23834	60	1154,3	6,437616
#17	Soil heat flux 10cm [MJ/m2] #1	-0,8184356	0,8976205	0,1286816	60	7,720897	0,4065697
#18	Wind direction [deg]	64,45747	281,388	178,3178	60	10699,07	56,23433
#19	Wind speed [m/s]	0,7698811	3,153821	1,50383	60	90,22982	0,5910707
#20	VPD up [hPa]	2,157675	19,63957	7,62999	60	457,7994	3,643272
#21	Air humidity up [hPa]	10,78989	21,93376	16,00194	60	960,1164	2,892862
#22	VPD dn [hPa]	1,938559	18,73337	7,58734	60	455,2404	3,564592
#23	Air humidity dn [hPa]	11,23103	22,28531	16,41665	60	984,9989	2,992548
#24	dT [deg.C]	-0,2431216	1,054115	0,06824385	60	4,094631	0,2212575
#25	de [hPa]	0,02603902	1,515804	0,414708	60	24,88248	0,3078871
#26	Bowen ratio	0,4503553	1,561781	0,8317174	54	44,91274	0,2212126
#27	ET [mm/d]	1,318432	5,066604	3,127892	31	96,96464	0,7830321
#28	PET Penman I.part [mm]	0,3282768	5,68379	3,760714	60	225,6428	1,358487
#29	PET Penman II.part [mm]	0,3862103	1,695415	1,027687	60	61,66124	0,3031222
#30	PET Penman [mm/d]	0,9865422	7,14452	4,788401	60	287,3041	1,57063
#31	PET FAO I.part	0,2325357	5,225543	3,224797	60	193,4878	1,288331
#32	PET FAO II.part	0,3247219	1,559859	0,9105872	60	54,63523	0,2935378
#33	PET FAO [mm/d]	0,8204274	6,374952	4,135384	60	248,123	1,412099
#34	ET filled [mm/d]	0,8139613	5,962545	3,260127	60	195,6076	1,168616

Table 8.3.4a) 24-hour interval statistics of the whole set of variables - 1st part.

#35	CH1 [mm/d]	0,9830125	10,52899	5,495781	44	241,8144	2,441704
#36	CH2 [mm/d]	0,8644126	8,241364	3,916036	44	172,3056	1,767914
#37	CH3 [mm/d]	0,727464	7,25844	3,62592	44	159,5405	1,71553
#38	CH4 [mm/d]	0,683696	6,504537	3,272486	43	140,7169	1,569693
#39	CH5 [mm/d]	0,6611568	7,98114	4,052067	44	178,291	1,772904
#40	CH6 [mm/d]	0,181352	5,169705	2,50394	43	107,6694	1,235328
#41	CH7 [mm/d]	0,7697613	8,684719	4,296559	44	189,0486	1,836216
#42	CH8 [mm/d]	0,1391526	7,477232	2,608135	42	109,5417	2,14271
#43	CH9 [mm/d]	0,7704641	7,007827	3,783923	43	162,7087	1,49133
#44	CH10 [mm/d]	1,036904	9,318114	5,263187	44	231,5802	2,209388
#45	CH11 [mm/d]	1,187533	8,321042	4,757361	44	209,3239	1,726531
#46	CH12 [mm/d]	1,147059	6,763125	3,684189	44	162,1043	1,234154
#47	Global rad. [MJ/m2] #2624	2,338962	27,77696	19,23834	60	1154,3	6,437616
#48	VPD up [hPa]	2,157675	19,63957	7,62999	60	457,7994	3,643272
#49	VPD dn [hPa]	1,938559	18,73337	7,58734	60	455,2404	3,564592
#50	CH1 calc [mm/d]	0,1773054	11,37615	4,863705	60	291,8223	2,857955
#51	CH2 calc [mm/d]	0,1342604	8,713745	3,685275	60	221,1165	2,178945
#52	CH3 calc [mm/d]	0,1665876	10,64828	4,566739	60	274,0043	2,67854
#53	CH4 calc [mm/d]	0,09628639	6,656801	2,721219	60	163,2731	1,646294
#54	CH5 calc [mm/d]	0,1297219	8,565699	3,52345	60	211,407	2,113834
#55	CH6 calc [mm/d]	0,07777039	5,3792	2,223678	60	133,4207	1,338645
#56	CH7 calc [mm/d]	0,1345557	8,623994	3,68216	60	220,9296	2,164624
#57	CH8 calc [mm/d]	0,1120742	7,311124	3,106197	60	186,3718	1,834084
#58	CH9 calc [mm/d]	0,1304035	8,234408	3,536246	60	212,1748	2,069681
#59	CH10 calc [mm/d]	0,1768496	11,11969	4,781027	60	286,8616	2,795242
#60	CH11 calc [mm/d]	0,1792391	10,54907	4,688436	60	281,3062	2,679308
#61	CH12 calc [mm/d]	0,1155422	6,835762	2,999656	60	179,9793	1,724715
#62	DPT dn [°C]	8,608297	19,21918	14,14017	60	848,4104	2,780463

Table 8.3.4b) 24-hour interval statistics of the whole set of variables - 2nd part.

8.4 Photos

Photo 8.4.1: Bowen-ratio sensor installed in corn field (©Pivec, 2013).

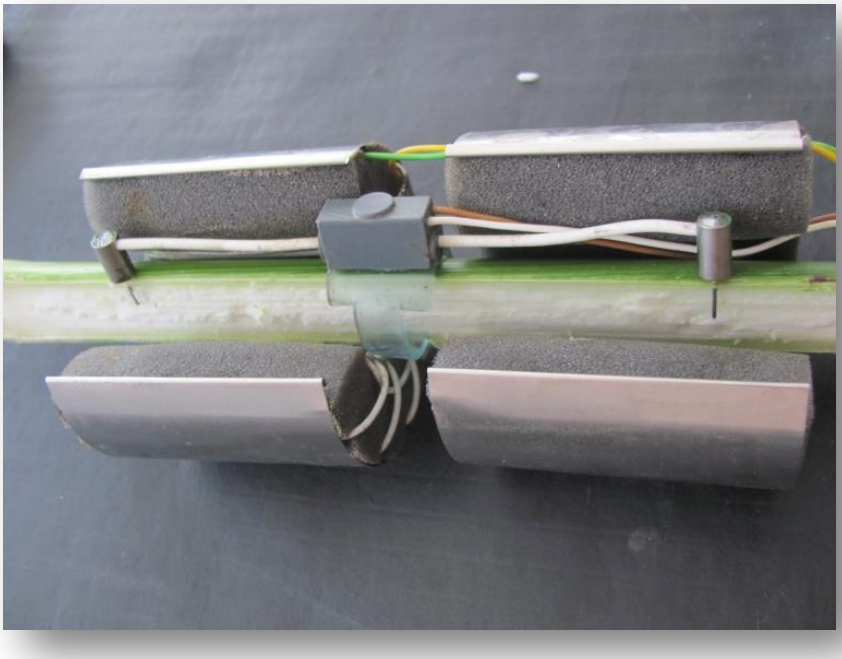

Photo 8.4.2: Cross-section of sap-flow sensor plugged into the stem (©Brant, 2013).

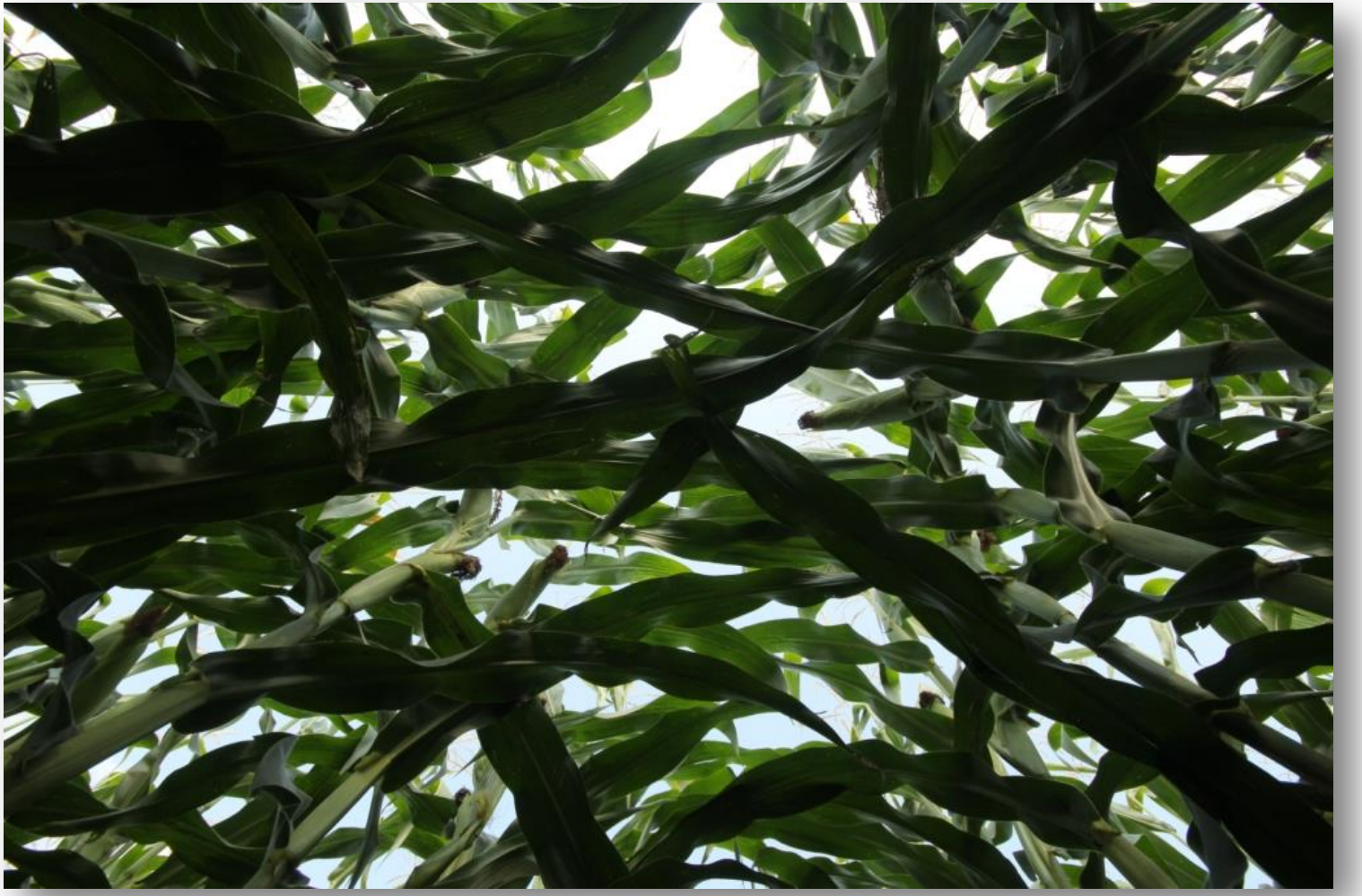

Photo 8.4.3: Light penetration into the corn canopy (©Hamouz, 2013).

9 Bibliography

Printed monographic publications and articles:

Allen R.G., Pereira L.S, Raes, D., Smith, M. 1998. Crop evapotranspiration – Guidelines for computing crop water requirements - FAO Irrigation and drainage paper 56 – Food and Agriculture Organization of the United Nations, Rome, 1998

Bot, A., Benites, J. 2005. Drought-resistant Soils: Optimization of Soil Moisture for Sustainable Plant Production : Proceedings of the Electronic Conference Organized by the FAO Land and Water Development Division, Volume 1 Food & Agriculture Org.

Bowen, I. S. 1926. The ratio of heat losses by conduction and by evaporation from any water surface. Phys. Rev. 27, p. 779-787.

Brant, V. 26th March 2014. pers. comm.

Brutsaert, W. 1982. Evaporation into the Atmosphere: Theory, History and Applications, 299 pp.

Campbell, N. A., Reece, J.B. 2006. Biologie. (Authorized translation from the English language edition, entitled Biology, 6th edition, published by Pearson Education, Inc., publishing as Benjamin Cummings 2002). Computer press, a. s. ISBN 80-251-1178-4 a) p.43-45,b) p.478, c) p.450-452, d) p.754-761,e) p.191-192.

Cohen, Y., Li, Y. 1996. Validating sap flow measurement in field-grown sunflower and corn. J. of Experimental Botany, vol. 47, no. 304, p. 1699-1707.

Cowan, I. R. 1982. Regulation of water use in relation to carbon gain on higher plants. In: Lange, O. L., et al. (Eds.), Physiological Plant Ecology II. Springer, Berlin, Germany, p. 589-614.

Čermák, J., Cienciala, E., Kučera, J., Lindroth, A., Bednářová, E. 1994. Individual variation of sap-flow rate in large pine and spruce trees and stand transpiration: a pilot study at the central NOPEX site. J. of Hydrology 168 (1995), p.17-27.

Čermák J.; Kučera, J. & Nadezhdina, N. 2004. Sap flow measurements with some thermodynamic methods, flow integration within trees and scaling up from sample trees to entire forest stands. Trees, Vol. 18, No. 5, p. 529–546, ISSN 0931-1890

Gallagher, J. N., and Biscoe, P.V. 1978. Radiation absorption, growth, and yield of cereals. J. Agric. Sci. 91:47-60.

Hatfield, J. L. 1990. Methods of estimating evapotranspiration. In B.A. Stewart and D.R. Nielsen (ed.) Irrigation of agricultural crops. Agron. Monogr. 30. ASA, CSSA, and SSSA, Madison, WI, p. 435-474.

Jara, J., Stockle, C. O., Kjelgaard, J. 1998. Measurement of evapotranspiration and its components in a corn (*Zea Mays L.*) field. Agric. Forest Meteorol. 92, p. 131-145.

Jones, H. G. 1980. Interaction and integration of adaptive responses to water stress: The implications of an unpredictable environment. In: Turner, N. C., Kramer, P. J., (Eds.), Adaptation of Plants to Water and High Temperature Stress. Wiley, New York, p. 353-365.

Kjelgaard, J. F., Stockle, C. O., Black, R. A., Campbell G.S. 1997. Measuring sap flow with the heat balance approach using constant and variable heat inputs. Agric. Forest Meteorol. 85, p. 239-250.

Köstner, B., Biron, R., Siegwolf, R., Granier, A. 1996. Estimates of Water Vapour Flux and Canopy Conductance of Scots Pine at the Tree Level Utilizing Different Xylem Sap Flow Methods. Theor Appl. Climatol. 53, p. 105-113.

Kustas, W.P., Stannard, D.I., Allwine, K.J. 1996. Variability in surface energy flux partitioning during Washita ’92: Resulting effects on Penman-Monteith and Priestley-Taylor parameters. Agric. For. Meteor. 82, p. 181-193.

Labedzki, L., Kanecka-Geszke, E., Bak, B., Slowinska, S. 2011. Estimation of Reference Evapotranspiration using the FAO Pentman-Monteith Method for Climatic Conditions of Poland, published by InTech; Printed edition published in March 2011, ISBN 978-953-307-251-7

McCree, K. J. 1972. Test of current definitions of photosynthetically active radiation against leaf photosynthesis data. Agric. Meteorol. 10, p. 443-453.

Merta M., Sambale, Ch., Seidler, Ch., Peschke, G. 2001. Suitability of plant physiological methods to estimate the transpiration of agricultural crops. *J. Plant Nutr. Soil Sci*. 164, p. 43-48.

Monteith, J. L. 1977. Climate and the efficiency of crop production in Britain. *Philos. Trans. R. Soc. London B* 281, p. 277-294.

Otegui, M. E., Nicolini, M. G., Ruiz, R. A., and Dodds, P. A. 1995. Sowing date effects on grain yield components of different maize genotypes. *Agron. J.* 87:29-33.

Perez, P.J., Castellvi, F., Rosell, J.I., Ibanez, M. 1999. Assessment of reliability of Bowen ratio method for partitioning fluxes. Agric. For. Meteorol. 97 (3), 141-150.

Peschke, G. K., Kaufmann, K., Sambale C., Töpfer, J., Zimmermann, S. 1997. Liefern Verfahren der Künstlichen Intelligenz nützliche Ergänzungen zur traditionellen hydrologischen Modellierung? In G.H. Schmitz (ed.): Modellierung in der Hydrologie. TU Dresden, Tagungsband des Symposiums in Dresden, 28-38.

Phillips N.G., Oren, R., Licata, J., Linder, S. 2004. Time series diagnosis of tree hydraulic characteristics. Tree Physiol. 24:879-890.

Phillips N.G., Scholz, F.G., Bucci, S.J., Goldstein G., Meinzer F.C. 2008. Using branch and basal trunk sap flow measurements to estimate whole-plant water capacitance: comment on Burgess and Dawson (2008). Plant Soil (2009) 315:315-324

Pivec J., Brant V., Moravec D. 2006. Analysis of the potential evapotranspiration demands in the Czech Republic between 1961–1990. Biologia 61(19): 294–299.

Pivec J., Brant V. 2008. The Actual Consumption of Water by Selected Cultivated and Weed Species of Plants and the Actual Values of Evapotranspiration of the Stands as Determined Under Field Conditions, Hydrology of Small Basin, Prague; Soil & Water Res. 4, 2009 (Special Issue 2)

Prueger, J. H., Hatfield, J. L., Aase, J. K., and Pikul, Jr., J. L. 1997. Bowen-Ratio Comparisons with Lysimeter Evapotranspiration. Reprint from Agronomy Journal Vol. 89, No. 5.

Rampazzo, N. 2013. Pers. comm.

Rooney, L. W., and Suhendro, E.L. 2001. Food quality of corn. In E. Lusas and L. W. Rooney (eds.), Snack Foods Processing, Technomic Publishing, Lancaster, PA, pp. 39-71.

Sinclair, T. R., Bennett, J.M., and Muchow, R.C. 1990. Relative sensitivity of grain yield and biomass accumulation to drought in field-grown maize. Crop Sci. 30:690-693.

Smith, C. W., Bertrán, J., Runge, E. C. A. 2004. Corn: origin, history, technology, and production, Wiley Series in Crop Science, ISBN 0-471-41184-1.

Stannard, D. I. 1996. A theoretically based determination of Bowen-ratio fetch requirements. U.S. Geological Survey, Denver, Colorado, U.S.A.

Steduto, P., Hsiao, T. C. 1998. Maize canopies under two soil water regimes IV. Validity of Bowen ratio-energy balance technique for measuring water vapor and carbon dioxide fluxes at 5-min intervals. Agri. and Forest Meteorol. 89, 215-228.

Von Willert, J., Matyssek, R., Herppich W. 1995. Experimentelle Pflanzenökologie, Grundlagen und Anwendungen. Georg Thieme Verlag Stuttgart, New York, S. 344.

Woodward, F. I., Sheehy, J. E. 1983. Principles and Measurements in Environmental Biology. Butterworth & Co., Ltd., London.

Yu, G.-R., Nakayama, K., Matsuoka, N., Kon, H. 1998. A combination model for estimating stomatal conductance of maize (*Zea mays L.*) leaves over a long term. Agric. Forest Meteorol., 92, 9-28.

Zhang, J., Xiangzhen, S., Bin, L., Baolin, S., Jianmin, L., Dianxi, Z. 2001. An improved water-use efficiency for winter wheat grown under reduced irrigation. Field Crops Research 59, 91-98.

Electronical sources:

Dictionary of Biology - Online encyclopedia 2014. <http://www.encyclopedia.com/doc/1O6-pressurepotential.html> [cited March 30, 2014]

Environmental Measuring Systems Brno http://www.emsbrno.cz

Hukseflux Thermal Sensors <http://www.hukseflux.com/>

Meteoservis v.o.s. http://www.meteoservis.cz/

Northeast Region Certified Crop Adviser (NRCAA) Study Resources 2010 Cornell University available online http://nrcca.cals.cornell.edu/

Reverse Osmosis Chemicals International – Reverse Osmosis Guide. 2013. Available from: <http://www.reverseosmosischemicals.com/reverse-osmosis-guides/reverse-osmosis-glossary-terms/flux-water-flux-reverse-osmosis-systems> [cited January 31, 2014]

University of British Columbia, Canada; Faculty of Land and Food Systems, Online source: <http://www.landfood.ubc.ca> [cited January 8, 2014]

U.S. – Geological Survey. <http://water.usgs.gov/edu/watercycle.ht>, [cited March 10, 2014] and <http://pubs.usgs.gov/of/2006/1312/figure8.html> [cited March 10, 2014]